PAUL SCHERRER INSTITU	T	SLS 2.0
Titel /Title	SLS 2.0 Baseline Lattice	Dokument Nummer / Document Identification SLS2-SA81-004-17
Autor(en) / Author(s)	A. Streun, M. Aiba, S. Bettoni, M. Böge, B. Riemann, V. Schlott	18.11.2021

Summary

This note is just an excerpt from the Technical Design Report plus modification history.

It includes lattice design, booster-to-ring transfer line and commissioning, and thus replaces or [partially] updates following documents:

SLS2-SA81-004-16_Lattice, SLS2-SA81-008-5_BRTL, SLS2-SA81-007-9_Magnets.

TDR lattice version is B069.

Table of contents

Modification History	2
Introduction	
The lattice concept	
The 7-Bend achromatic arc	6
Straight sections	
Undulator portfolio and source parameters	
Radio-frequency bucket	
Non-linear optics	13
Tuning range and correction capability	
Magnet specifications	
Injection concept	
Real lattice performance	22
Booster to ring transfer line (BRTL)	
Commissioning	
References	

Modification History

Version 004-17 (18.11.2021) - Lattice B069

• This update is required to adjust *this* note to the TDR.

Version 004-16 (3.12.2020) - Lattice B066

• Based on the meetings on injection element in Nov. 2020, new parameters for the septa are assumed, leading to the layout B066. These changes affect only straight 1L.

Version 004-15 (12.10.2020) - Lattice B064

• Following design change request DCR-SLS2-VV84-001-0 the magnets AN, ANM, BEV and BEH|BES are not rotated (equal edge angles) but installed such, that the edges facing the adjacent SOQ and SXQ magnets are parallel to these. This does not change the orbit and with it the "Heilige Liste". Changes of the optics are tiny and not visible in plots, therefore nothing has been changed in this note. Nevertheless the optics had to be retuned thus creating Lattice B064.

Version 004-14 (1.9.2020) – Lattice B063

- Based on the layout meeting from Aug. 13, 2020 the split ratio of the medium and long straights and the insertion devices portfolio was defined.
- Superbend field profiles updated.
- Layout of injecton straight confirmed.
- Quadrupoles in two mirror symmetric versions

Version 004-13 (18.6.2020 [25.6.2020 typos corrected]) – Lattice B062

- Re-introduced medium straights with lattice version B057 in order to minimize the radial shifts of beam lines, such that they all pass the existing openings in the tunnel front walls.
- Modified optics of dispersion suppressor section for higher brightness.
 - o As a consequence, introduction of a new magnet VBX and modification of ANM.
 - o Modification of dispersion suppressor magnes BEV and BE.

Version 004-11/12 (3.3.2020) – Lattice B046 (which is almost identical to B039)

- Increased energy to 2.7 GeV
- Abandoned "phase 2" due to infeasibility with regard to dynamic aperture.
- Return to QA-SLS type quads of 20 cm length in injection straight.
- Included new superbend designs (C. Calzolaio, 10.2.20202) for 2.7, 4.0, 5.0 T for 2.4 GeV, used 2.7 and 4.0 T fields for scaling to approx. 2.4/3.5/5.0 T
- Keeping QPH for smaller betas in straights, although no feasible DA found yet.
- Return to horizontal injection scheme

Version 004-10 (28.11.2019) - Lattice B039/B139

- Established injection straight layout for phase 1 and phase 2. This required to change two quad types in injection straight.
- The standalone sextupole in the dispersion suppressor actually will become a modified sextupole (SXQ) with elliptic or enlarged aperture.

Version 004-9 (10.10.2019) – Lattice B038/B138

A modification of the dispersion suppressor region was required to obtain sufficiently large stay
clear apertures for outcoupling of photon beams. Compound magnet BE was split into two parts
BEV and BEH with a standalone sextupole (SDM) between. The octupole (OCYM) was
removed.

Version 004-8 (25.9.2019) – Lattice B036/B136

- Including injection straight design
- Vacuum chamber design (space for flanges!) required minor changes of distances/lengths for BPMs/Correctors [in mm]:

SLS2-SA81-004

- o new: 12.5 25 (BPM) 23 105 (Corr) 4.5 (dist to adjacent SOQ)
- o prev.: 15 20 (BPM) -15 110 (Corr) -10 (dist to adjacent SOQ)
- Modification of quad types mag. length and max. gradient
 - o QP : 120 mm / 80 T/m \rightarrow 100 mm / 92 T/m
 - $\circ \quad \text{QPH: } 120 \text{ mm} / 105 \text{ T/m} \rightarrow 140 \text{ mm} / 100 \text{ T/m}$
 - → Wider tuning range for split standard straights and smoother optics
- Modification of main bend BN: longitudinal gradient replaced by homogenous bend.
 - this caused tiny changes of layout (microns) and AN, VB parameters (<10⁻³)
- Replaced doublett in long straight by triplett
- Redesign of injection straight for vertical injection

Version 004-7 (19.07.2019) – Lattice B025-125

- Update/rewrite for completely new lattice of type "B+"
- Magnet specs moved out to note SLS2-SA81-007-1

Previous modifications are irrelevant now but may be looked up in SLS2-SA81-004-6 OUTDATED.

Introduction

This chapter describes the layout, parameters and optics of the lattice. Changes compared to a previous version, which had been adopted as reference in June 2020, and to subsequent versions are marginal. Therefore, results in other chapters of this TDR based on these previous versions are still valid.

For the purpose of the technical design, the relevant specifications are mainly found under 'straight sections', 'radio frequency' and 'magnets'.

The lattice will be realized in two phases, "Phase 1" with four permanent magnet superbends, and "Phase 2" with two of these replaced by variable superconducting magnet superbends. The calculations described in this chapter are based on Phase 2, unless otherwise stated.

The lattice concept

The lattice design was made with the following goals and constraints in mind:

- a) An increase of brightness in the hard X-ray regime, by at least a factor of 40, compared to the existing SLS storage ring.
- b) Extend the hard X-ray range of dipole beamlines to higher energy (~60 keV)
- c) Higher photon flux for soft and tender X-ray (spectroscopy) beamlines.
- d) Higher coherent flux for ptychography beamlines.
- e) Maintain the performance of the present SLS in the VUV range (~20 eV).
- f) Follow closely the geometric footprint of the existing storage ring in order to avoid modifications of the tunnel and minimize the shifts of photon beam source points.
- g) Maintain a beam lifetime in the range of about 10 hours to meet radiation protection regulations.
- h) Provide sufficient storage ring acceptance to enable top-up injection with the existing SLS injector.

The following features of the new lattice fulfill the design charge:

- (1) Twelve 7-bend-achromatic arcs of about the same length replace the twelve triple-bend achromatic arcs of the existing lattice in order to reduce the natural emittance.
- (2) A novel unit cell, combining a longitudinal gradient bend with reverse bend magnets, is employed to reduce the natural emittance still further.
- (3) The beam energy is increased from 2.4 GeV to 2.7 GeV to shift the undulator harmonics to higher photon energy and to increase the flux.
- (4) The beam current is maintained at 400 mA in order to not lose in flux.
- (5) Superbend magnets with higher peak field (2.1... 5.4 T) are integrated into the arcs to provide hard X-rays.
- (6) The lattice has three long, three medium and six short straight sections like the existing storage ring to closely follow its geometric footprint.
- (7) Despite the 3-fold lattice geometry, the non-linear optics is tuned to 12-fold symmetry in order to maximize the storage ring acceptance.
- (8) The electron beam is focused in the straight sections with some compromise due to constraints from non-linear optics in order to minimize the photon beam emittance as obtained from the convolution of the electron beam properties with diffraction.

The new type of arc (1) and the novel unit cell (2) reduce the natural emittance by a factor 45. The increase of energy (3) and the matching to the straight sections (8) still results in a factor 24 decrease of the hard-X-ray (10...20 keV) effective photon beam emittance. The increase of flux due to the higher energy (3) and maintaining the current (4) would result in almost a factor 60 increase of hard-X-ray brightness if the existing undulators were re-used. However, new undulators of smaller period will finally increase the brightness by factors >100 at 10 keV and up to a factor 1000 above 20 keV (see the chapter on "Sources" in this TDR).

Due to the high field superbends (5) and higher beam energy (3), the useful energy range of dipole beam lines is extended to about 80 keV. Following closely the existing footprint (6) avoids tunnel modifications and keeps the lateral source point shifts within ±70 mm of their present positions, so the photon beam pipes pass the existing front-wall apertures. Large dynamic storage ring acceptances based on high optics symmetry (7) enable classical off-axis injection schemes, leaving more advanced schemes as a possible future upgrade option but not as necessity, and provide a beam lifetime of about ten hours.

As stated above, the new lattice will have three long, three medium and six short straight sections in order to follow closely the existing footprint and minimize modifications of the ring tunnel. The overall straight length is slightly increased.

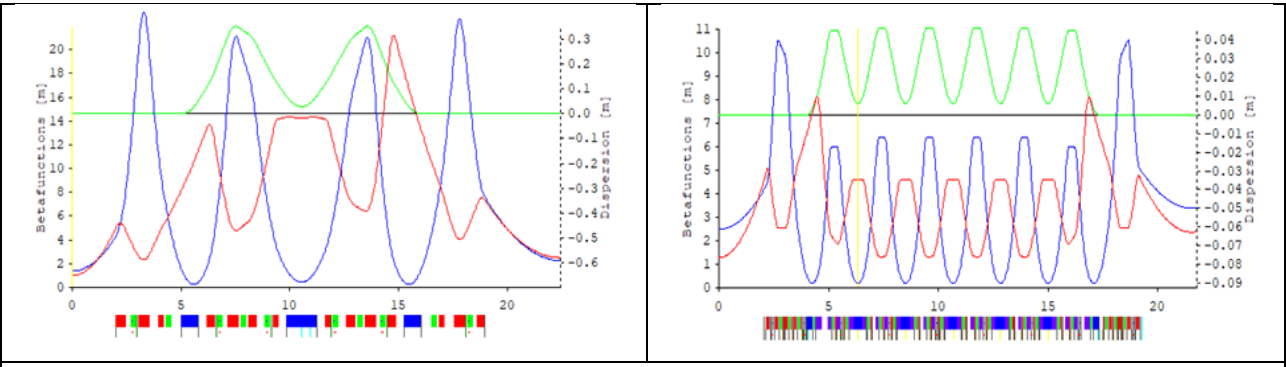


Figure 1: optical function in one arc (from short to medium straight) for the existing (left) and the new (right) lattice (β_x , β_y , η_x). Note the different scales.

Figure 1 gives a comparison of the optical functions in one arc for the old and the new lattice, and Table 1 compares the most important lattice parameters of the existing lattice, the lattice presented in the Conceptual Design Report (CDR), and the final new lattice.

Table 1 Comparison of the most important parameters of the existing lattice (including FEMTO insertion), of the lattice presented in the Conceptual Design Report (both including three superbends) and the final lattice including the "Phase 2" set of four superbends.

	SLS today	SLS 2.0 CDR	SLS 2.0 TDR
Lattice type	TBA	7-BA	7-BA
Circumference [m]	288	290.4	288
Periodicity (arc geometry)	3	12	3
Energy [GeV]	2.411	2.400	2.700
Beam current [mA]	400	400	400
Natural emittance [pm.rad]	5630	102	158
Energy spread [10 ⁻³]	0.88	1.03	1.16
Radiation loss per turn [keV]	549	554	688
Momentum compaction factor [10 ⁻⁴]	6.04	-1.33	1.05
Working point Q_x , Q_y	20.43, 8.74	39.20, 15.30	39.37, 15.22
Chromaticity ξ_x, ξ_y	-67.3, -21.0	-95.0, -35.2	-99.0, -33.4
Total gross straight length [m]	79.9	66.3	83.6
Vertical emittance in operation [pm.rad]	~5	10	10
Beam lifetime in operation [h]	~9		9.5

The main changes of the final lattice with respect to the lattice presented in the CDR are as follows:

- Energy increase to 2.7 GeV.
- 3-fold symmetry of the lattice layout (i.e. location of arcs).
- Three different types of straights, as in the existing lattice, and an increase of total available straight section length.
- Positive, instead of negative, momentum compaction to increase longitudinal instability thresholds and relax magnet parameters.
- Modification of the dispersion suppressor for extraction of VUV synchrotron radiation.

The 7-Bend achromatic arc

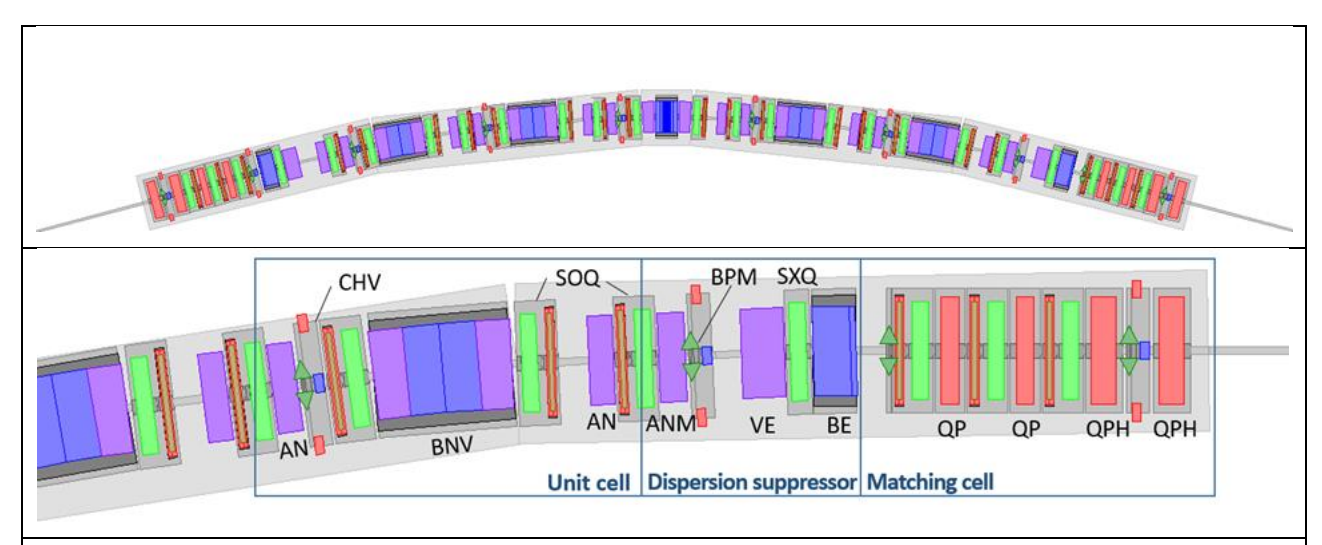


Figure 2: Schematic layout of an arc containing a central superbend, and a magnified view of the downstream end. Absorbers are not shown.

An arc as shown in Figure 2 contains seven main bending magnets. The center bend is placed on a plinth such that it can be replaced by a superbend while all other elements are on four girders. The arc is composed from five unit cells, two dispersion suppressor cells and two matching cells.

The five unit cells are identical (unless a superbend is installed) and provide a net deflection angle of 5° each. Each unit cell contains a BNV = {VB|BN|VB} composite dipole, where VB is a combined function magnet with vertically focusing gradient and BN is a simple dipole magnet. The composite dipole BNV represents a simple longitudinal gradient bend (LGB) of the "sandwich" type; the dipole field of BN is higher than that of VB.

The other essential component in the unit cell is a reverse bend (RB), AN. It is also a combined function bend as is VB but with horizontally focusing gradient. The LGB-RB combination was developed for SLS 2.0 to provide the lowest emittance. It realizes a natural emittance lower by a factor of about 4 with respect to a typical theoretical minimum emittance type lattice.

The dispersion suppressor cell is derived from a half unit cell, but the bending magnet is split into two parts, a combined function bend VE and a pure dipole BE with a sextupole SXQ of enlarged aperture between. This configuration was necessary to provide sufficient clearance for extraction of VUV photon beams from the straight section.

The VB magnet of the BNVs, and the AN reverse bends facing the dispersion suppressors are modified types, named respectively VBX and ANM, required for proper matching. This results in the following array of pure dipoles, combined function bend and reverse bends along one arc:

In addition to the bending magnets, which define the arc geometry, the arc contains further magnets and beam position monitors (BPMs). These are all necessary for tuning, controlling and correcting the optics as discussed below. In Figure 2, SOQ is a combination of a sextupole (SX) and an octupole (OC), where quadrupole and skew quadrupole functions (QA and QS) are integrated into the octupole OC by additional coils. Three SOQs are installed per unit cell. The element CHV represents the combination of a horizontal corrector (CH) and a vertical corrector (CV).

Note that BPM/CHV stations alternate with absorbers (not shown), i.e., the BPM/CHV pattern is not symmetric. The dispersion suppressor at the end of the arc contains a BPM/CHV station, whereas the one at the entry of the arc contains an absorber.

The matching sections are identical, independent of the type of straight that follows. The cell contains four quadrupoles (two short, QP, and two long, QPH) and three SOQs. The upstream cell contains two BPM/CHV stations, the downstream cell contains one BPM/CHV station and a single BPM combined with an absorber. The concept of "pseudo symmetry" is imposed on the optics along the matching sections and the straight sections as explained in the next section.

The center bends in arcs 01, 02, 06 and 10 will be replaced by superbends to provide hard-Xrays for the Debye, s-TomCat, PX-III and superXAS beam lines. In "Phase 1", all four will be permanent magnets with reduced gap and 2.1 T peak field. In "Phase 2" the bends in arcs 01 and 02 will be replaced by superconducting superbends, which can be varied in field between 2.8 T and 5.4 T.

The edge focusing effect of the superbend is different to that of the normal bend, so 2×5 tuning quadrupoles (QA) in the SOQ magnets of the three central arc cells (red squares in Figure 3) are used to adjust the arc tunes and restore the symmetry of the beta functions and dispersion. Although the perturbation of periodicity is almost invisible in Figure 3, it is sufficient to excite a non-systematic third integer resonance, and the lattice working point has to be set to avoid it.

Here, one assumes the same type of VB magnet as at the normal bends and the superbends, however it may be tuned in the laboratory beforehand to best match the superbend properties.

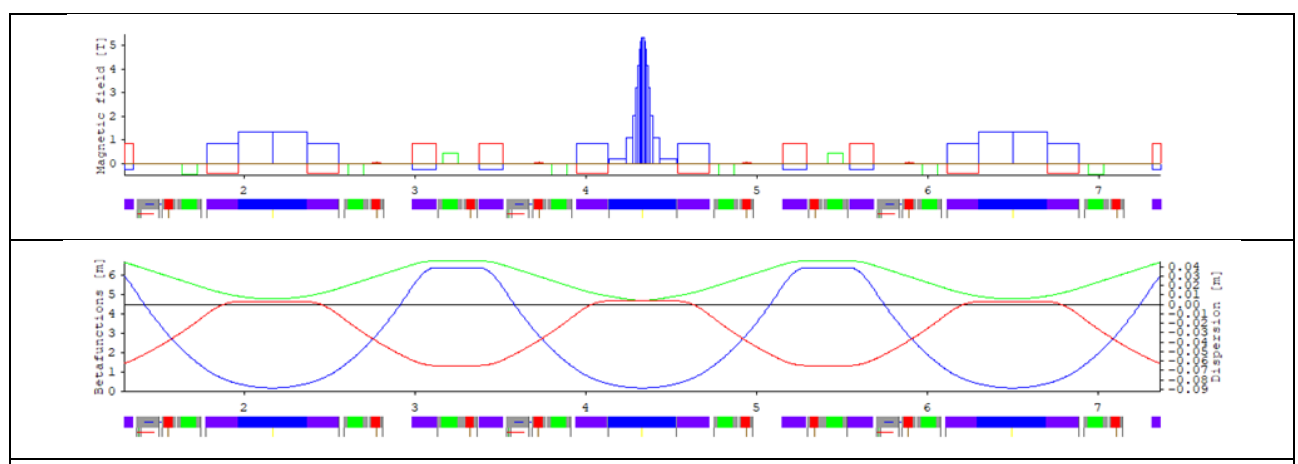


Figure 3: Pole-tip fields and optical functions in the arc containing a 5T superbend. Pole-tip fields B, B'R, $\frac{1}{2}$ B"R2 at a radius R = 11 mm.

Straight sections

The lattice has 12 straights, 6 short ones (even numbered sectors), 3 medium ones (sectors 3, 7 and 11) and 3 long ones, where two (sectors 5 and 9) are shared between experiments and RF-systems, while the third (sector 1) is required for injection.

Table 2 displays each straights gross length, net length, and radial and longitudinal shifts of the straight section midpoints, compared to the present locations.

- The total length is that between the end quadrupoles and includes the sector valves.
- The net length is that available for installation.
- A positive radial shift is towards the ring outside.
- A positive longitudinal shift is downstream (i.e. makes the beamline shorter).
- The shifts refer to the midpoints of the straights (total length).
- [Numbers in brackets refer to the midpoints of the usable straight (net lengths).]
- Bending magnets are included to complete the numbers on source points shifts.

The 12 arcs connecting the straight sections are identical and have a length of 17'030 mm between adjacent sector valves. The overall straight length is slightly increased as seen in Table 1.

Table 2: Straight section lengths and shifts compared to SLS today (all numbers in mm)

	SLS today		SLS 2.0				
Source	total length	total	net length	radial shift	long shift		
		length					
Long straights (1, 5, 9)	11730	12710	5000+6560°	+67.5	0 [-3755 / +2975] ^a		
Medium straights (3, 7, 11)	6970	6550	4980+820	+67.5	0 [-685]		
Short straights	3970	4310	4110	-2.15	0 [0]		
(2, 4, 6, 8, 10, 12)							
Bending magnets (all sectors)				-62.9 ^b	±135 ^c		

- a. refers to 1st and 2nd half of 5L. 9L is just the mirror image and injection straight 1L is different.
- b. radial shift for normal dipole. For superbend beam lines X01/02/06/10DA add 1.8/0.6/-0.8/-0.8 mm.
- c. positive for even numbered sectors, refers to the middle bend in the 7-BA arc.

High lattice symmetry is a prerequisite to establish large dynamic apertures, therefore the lattice maintains a 12-fold symmetry of the optical functions at the locations of non-linear elements (sextupoles, octupoles) although the geometry has only 3-fold symmetry and the linear optics, due to special optics at injection, has no symmetry at all. This constraint requires one to tune all straights irrespective of length and optics to exactly same the betatron phase advances.

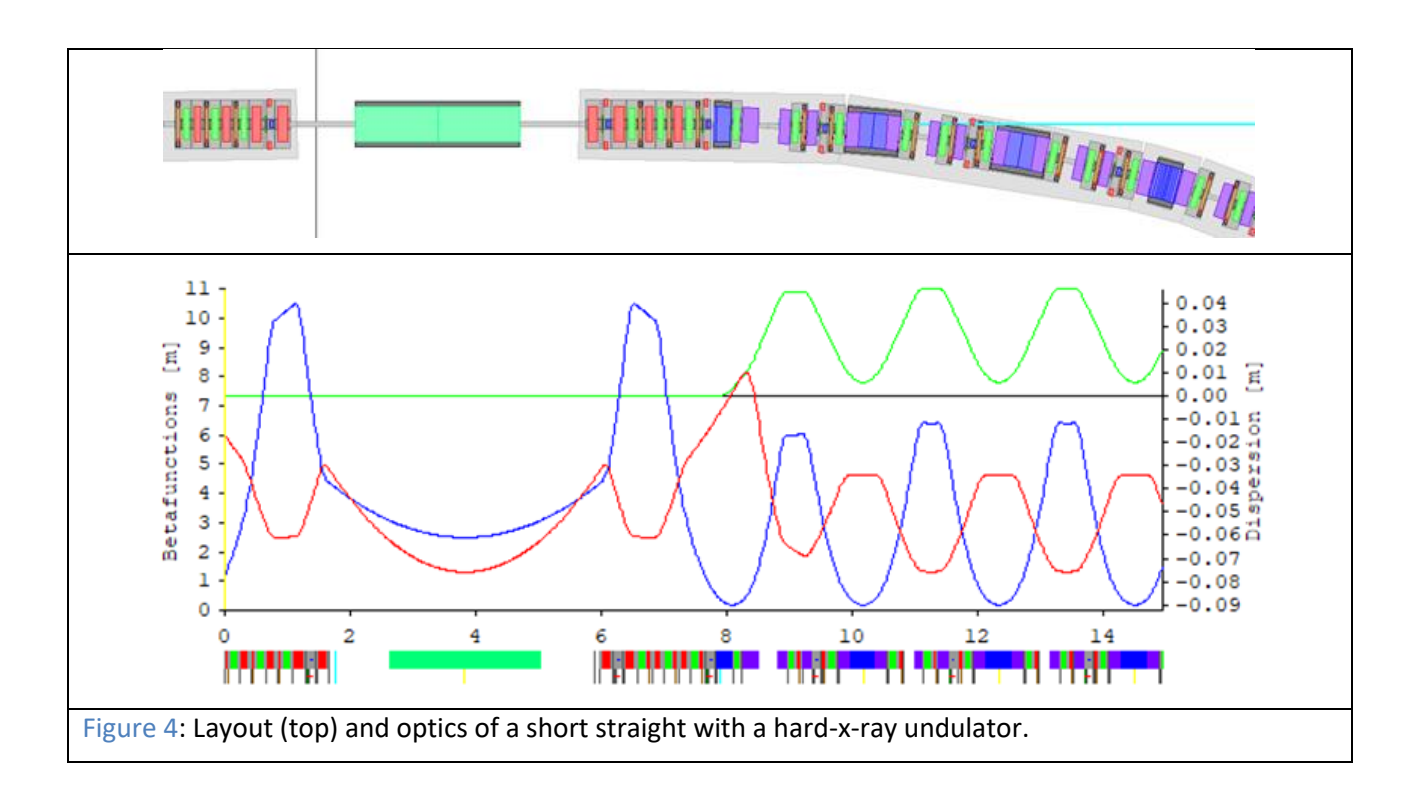
Starting with the short straight, four quadrupole pairs are used to set the two phases while maintaining symmetry ($\alpha_x = \alpha_y = 0$) at the center. Two of these pairs do not affect the optical functions at the last nonlinear elements, so they can be set differently in the other straights.

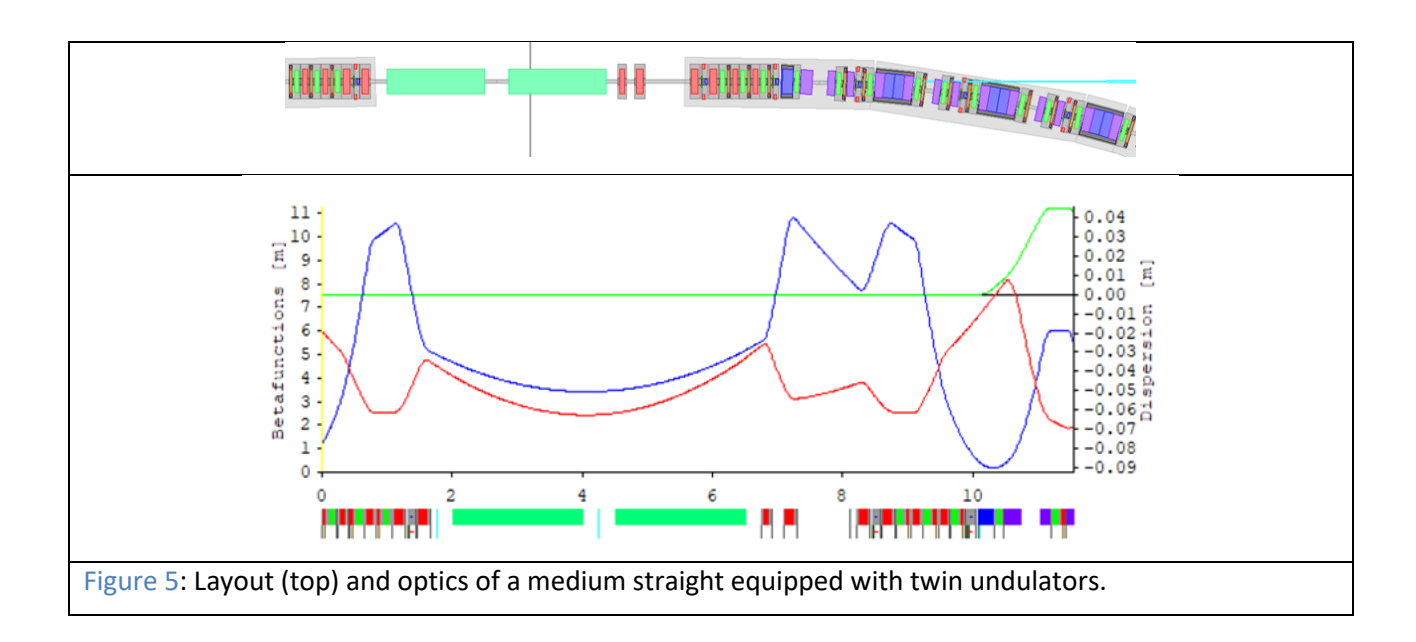
In the medium straight, the four quadrupoles from these two pairs plus two additional quadrupoles provide six degrees of freedom to maintain phases and preserve periodic continuation (β_x , β_y , α_x , α_y). As a consequence the medium straight is split by a doublet into a long part for undulator installation and a short part for machine equipment (e.g. multi-bunch feedback kicker).

In the same way the long straights 5 and 9 are split, but here two sub-straights of comparable lengths are created with a triplet instead of a doublet to get a more symmetric optics and another (redundant) degree of freedom.

The injection straight 1 is different: four large aperture quadrupoles (re-used from the SLS) are used to establish a telescope optics for magnification of dynamic aperture at the injection septum. The total 8 degrees of freedom are used to maintain phases, preserve periodic continuation and set α_x = 0 and a large β_x at the septum exit.

Figures 4 to 7 display schematic layouts and optics of the straights.





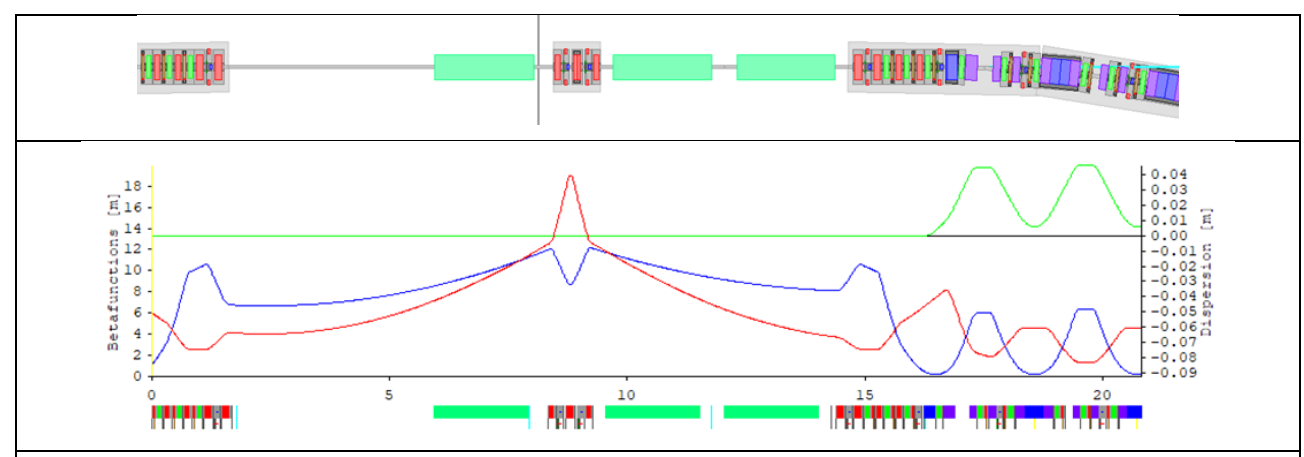
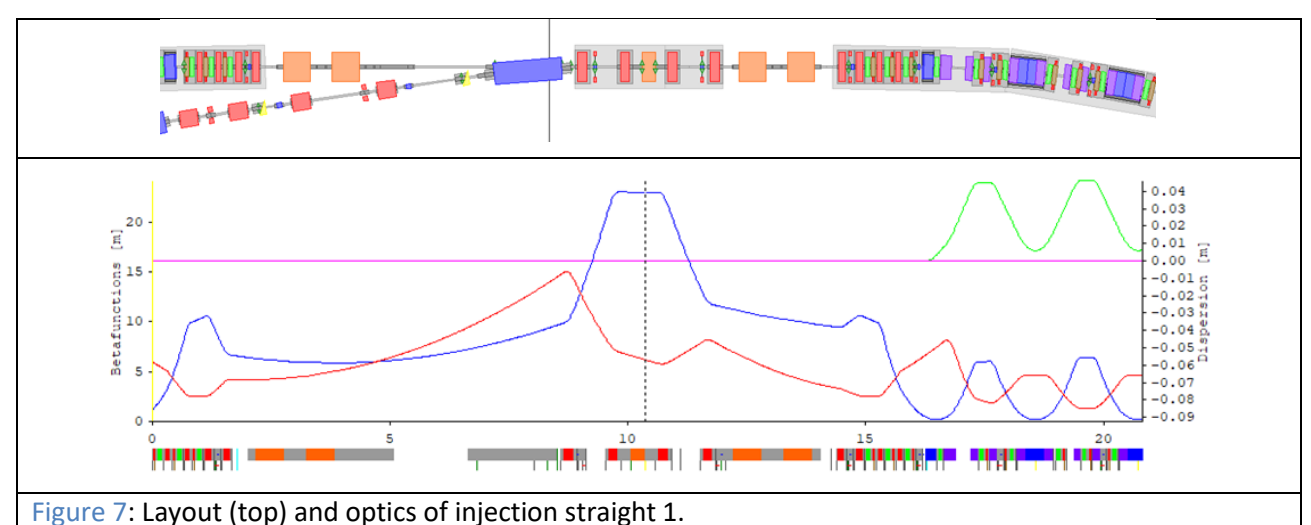


Figure 6: Layout (top) and optics of long straight 9L equipped with three VUV / soft-X-ray undulators. Straight 5L is the mirror image, with the shorter section upstream.



Orange boxes from left to right: kickers 1 and 2, thin septum, kickers 3 and 4.

Undulator portfolio and source parameters

For the lattice design calculations, the undulator portfolio from Table 3 is used. For more details, see chapter "Sources" of this TDR. The portfolio may be modified as the project progresses; however, this will not dramatically change the impact on the electron beam parameters.

The six short straights are equipped with planar undulators for hard X-rays. HTSU10 in 2S will be a superconducting undulator for the i-Tomcat beamline, to be installed in "Phase 2". CPMU14 in 4S is the (existing) cryogenic permanent magnet undulator of the material science beamline. Protein crystallography (PX-I, PX-II) and cSAXS in straights 6S, 10S, 12S get new U18 undulators, μ XAS in 8S a new cryogenic undulator CPMU16.

Soft x-ray beam lines are served by UE** Apple-X type undulators for variable polarization, where the max. K-values and respective peak fields can be realized in the horizontal or vertical dimension. In circular mode, the horizontal and vertical fields are same but of magnitude1/ $\sqrt{2}$ of the peak field. Phoenix/X-Treme in 7M will re-use the existing UE44 undulator. RIXS and SIM in mediums straights 7M, 11M as well as SX-ARPES in the second half of 5L get new UE36 twin undulators. An existing planar undulator U70 is located in the second half of 5L too for time-sharing operation of the lithography beamline XIL. The first half of 5L accommodates four fundamental RF cavities. The first half of 9L contains the twin 3rd harmonic cavities

and a single UE36 for the soft X-ray regime of the QUEST beamline, and the second half contains twin UE90 undulators to cover the VUV regime.

Table 3: "Phase 2" Insertion Device Portfolio. Total length includes tapers etc. Net length as used in the lattice files is just the product of period length and number of periods.

Straights	Undulator	Period	Length	N _{period}	Vacuum gap	K	B _{peak}
		[mm]	Total [m]		[mm]		[T]
2S	HTSU10	10	2.0	98	7.0 × 3.5	2.00	2.14
4S	CPMU14	14	2.3	120	4.0	1.50	1.22
85	CPMU16	16	3.5	185	4.0	2.00	1.34
6S/10S/12S	U18	18	3.5	164	4.0	2.12	1.26
7M	UE44	44	3.5	75	8.0	3.50	0.85
3M/11M/5Lb1	2×UE36	36	2×2.0	2×53	8.0 ∅	3.65	1.09
5L-b2	U70	70	1.5	21	9.0	4.80	0.73
9L-a2	UE36	36	2.0	53	9.0 ∅	3.65	1.09
9L-b	2×UE90	90	2×2.0	2×20	9.0 ∅	10.0	1.19

The undulators and superbends affect the equilibrium parameters of the storage ring. Table 4 gives parameters for the different project phases in comparison to the existing SLS.

- "Phase 1" is with four PM superbends of 2.1 T peak field.
- In "Phase 2", two of them in sectors 1 and 2 are exchanged for superconducting superbends, set to the maximum peak field of 5.4 T. For the insertion devices, it is assumed that they would all operate at minimum gap, which results in 90 kW radiated ID power at 400 mA.
- The values for the existing SLS are without IDs but include the three superbends (2.9 T peak field, in arcs 2, 6 and 10) and the FEMTO-chicane.
- The circumference of SLS was increased by 7.3 mm due to the installation of FEMTO, which caused 13 kHz frequency change. The total frequency change is 18 kHz compared to the original design frequency, this includes settlement of the building over the years. SLS2.0 will return to the original frequency for the circumference of 288.000 m. The four "Phase 2" superbends increase the circumference by 0.170 mm.
- Intra-beam scattering effects are rather small: the emittance increases by 2.6% and energy spread by 1.4% (400 mA beam current in 460 bunches, 3rd harmonic cavity for factor 3 bunch lengthening, 10 pm of vertical emittance).

Table 4: Equilibrium parameters with superbends and insertion devices

	SLS today	SLS 2.0					
		No SBs	"Phase 1"	"Phase 2"	+ IDs		
Circumference [m]	288.007'289	288.000'000	288.000'060	288.00	00'170		
Emittance [pm.rad]	5630	149	150	158	135		
Energy spread [10 ⁻³]	0.878	1.103	1.106	1.160	1.043		
Radiation loss [keV/turn]	549	666	668	688	915		
Hor. damping partition J _x	1.00	1.85	1.85	1.82	1.62		
Damping times x/y/E [ms]	8.4 / 8.4 / 4.2	4.2/7.8/6.8	4.2/7.8/6.7	4.1/7.5/6.4	3.5/5.7/4.1		

Table 5 gives the source beta function, size and divergence with emittance and energy spread from Table 4 / "Phase 2", and assuming 10 pm of vertical emittance. The source points of the bending magnets are located at the centers where $\alpha_x = \alpha_y = \eta_x' = 0$.

In the long straights, due to $\alpha \neq 0$ there is a correlation term $<\!xx'\!> = -\epsilon\alpha$ not shown in the table. The table gives only r.m.s. electron beam size and divergence, which has to be convoluted with the diffraction properties of the radiation source. In particular, for the bending magnets, the diffraction divergence completely dominates the electron beam divergence.

Table 5: Source size and divergence

Source	β _x [m]	β _y [m]	η _x [mm]	σ _x [μm]	σ _x ' [μrad]	σ _y [μm]	σ _y ' [μrad]
Long straights 5, 9 (middle of longer part)	7.75	5.87	0	35	4.9	7.7	1.6
Medium straights 3, 7, 11		2.40		23	6.8	4.9	2.1
Short straights 2, 4, 6, 8, 10, 12	2.50	1.28		20	7.9	3.6	2.78
Normal bending magnet, 1.35 T	0.18	4.6	5.8	8.6	30	6.8	1.5
Permanent magnet superbend, 2.1 T			5.4	8.2			
Superconducting superbend, 5.0 T			4.0	7.1			

Radio-frequency bucket

Without insertion devices, a total RF voltage of 1440 kV is required to provide a momentum acceptance of [-6.0%,+4.5%]. With all IDs closed to minimum gap, a voltage of 1715 kV would be required to maintain the same momentum acceptance.

Due to the substantial 2nd order momentum compaction the RF bucket becomes asymmetric as shown in Figure 8 for a main voltage of 1440 kV and a 3rd harmonic voltage of 375 kV, to lengthen the bunch by a factor 3 (to about 8.5 mm rms). Note that transition to alpha-bucket would already occur at 1835 kV.

Four 500 MHz RF cavities will be located in the first half of straight 5L. The passive superconducting 1.5 GHz twin cavities in a common cryostat are located in the first half of straight 9L.

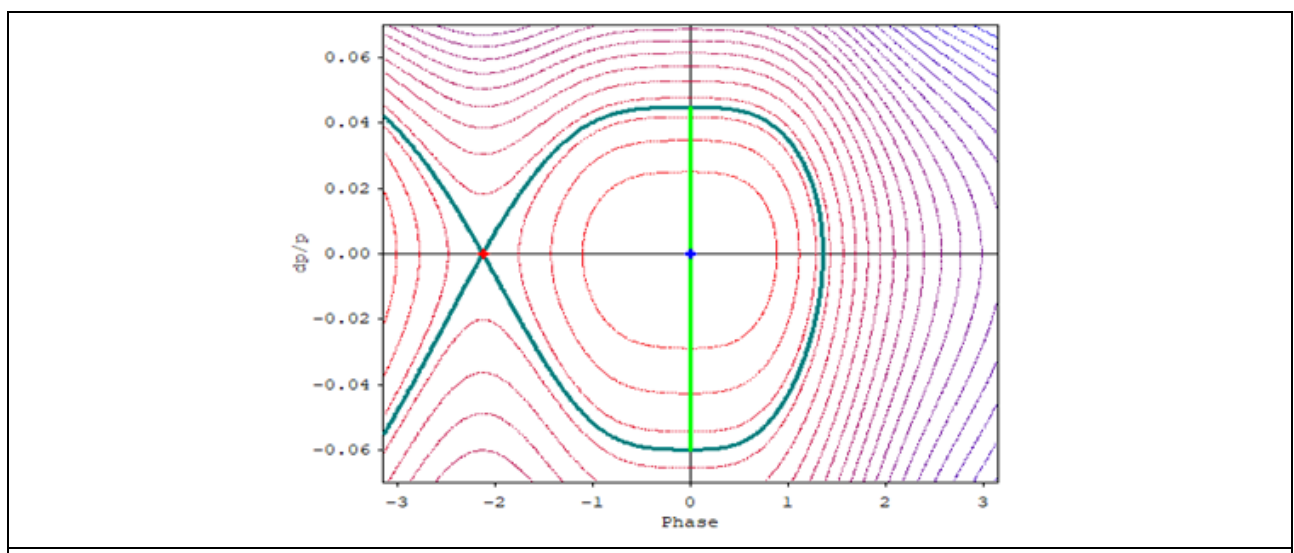


Figure 8: RF bucket including non-linear momentum compaction for 1440 kV fundamental and 375 kV 3rd harmonic voltage. The green bar indicates the momentum acceptance.

Non-linear optics

Optimization of non-linear optics is the greatest challenge for low emittance lattices. It enters the design from the very beginning and subsequently determines the structure of the arc and the emittance which can be achieved.

The natural chromaticity, due to momentum dependent of focusing, is adjusted by sextupoles in the dispersive regions, i.e. inside the arcs, to small, positive values in both planes. This is done in order to; (a) damp collective instabilities, in particular the dipole mode of the head-tail instability and transverse mode coupling instability due to the resistive-wall impedance, and (b) to confine the chromatic tune spread to a small region in tune space not overlapping with major resonances. While (a) works best with large positive chromaticity, (b) requires a small absolute value of chromaticity. A compromise is found around $\xi_x/\xi_y = +1/+1$.

Due to the small dispersion in the MBA lattice the sextupoles are rather strong, and since they are non-linear, particle motion becomes chaotic or unbounded beyond some amplitude, called dynamic aperture (DA). Sufficient DA is required for feasibility, the efficiency of injection, and sufficient momentum acceptance (MA). Sufficient MA, which is essentially off-momentum DA, is required to provide sufficient beam lifetime with regard to Touschek scattering.

The following means and methods of optics design were applied:

- A classical MBA with interleaved sextupoles was chosen instead of the hybrid-MBA (HMBA) based on the –I transformer configuration. The HMBA as developed for ESRF-EBS [1.01], and adopted at other places, provides superior on-momentum DA, but lower MA (i.e. off-momentum DA) due to coherent amplification of chromatic half-integer resonance drive terms (CHIRDT). Due to the rather low beam energy of SLS2.0, where Touschek scattering dominates beam lifetime, priority was given to obtaining large (±4%) MA provided that DA was sufficiently large for off-axis injection. Recent developments on a modified HMBA with larger MA [1.02] were discussed but did not reach maturity in time to be further considered.
- An MBA-arc with M=7 was chosen as the best compromise between low emittance (roughly scales with $(M-1)^{-3}$) and large DA. At unit cell tunes of $\{0.429, 0.143\} \approx \{3/7, 1/7\}$ all 1st and 2nd order, and even some 3rd order sextupolar resonance drive terms cancel out over seven cells [1.03]. However, this requires one to include "harmonic" sextupoles in the matching sections into the cancellation pattern.
- Due to the absence of dispersion in the matching sections and due to perturbation of the ideal cancellation pattern in order to suppress 2nd order effects such as amplitude dependent tune shifts (ADTS), fractional arc tunes near ½n + ¼, with n integer, help in suppression of the CHIRDTs. This is a prerequisite to achieve large MA. For the nominal optics, arc tunes are {3.28, 1.27}, close to {3¼, 1¼}.
- All DLSRs have a rather high periodicity in order to suppress most resonances due to symmetry. The SLS 2.0 lattice has only a period-3 geometry and period-1 linear optics, but the optical functions at all non-linear elements show period-12 symmetry. This is achieved by tuning all straights, irrespective of length and linear optics, to exactly same betatron phase advances, as mentioned in 'Straight Sections'. As a consequence the M-straights needed the insertion of a quadrupole doublet to realize the required degrees of freedom.
- Second-order sextupole effects like ADTS, 2nd order chromaticity and octupolar resonances cannot be well suppressed with the sextupoles alone. Octupoles are also needed to perform this task to 1st order. Therefore, most sextupoles are combined with octupoles in the so-called SOQ mangets.
- The lattice is equipped with 264 SOQ-magnets (22 per arc), each one containing a sextupole and an octupole. Due to space requirements for extracting VUV photon beams, 24 stand-alone sextupoles SXQ of larger aperture are used in the dispersion suppressor, and so octupoles are omitted there (Figure 2).

Figures 9A and 9B show the on-momentum DA at the exit of the thin injection septum for the ideal lattice without and with (ideal) the insertion devices from Table 3. Figure 9D is, like 9B, with IDs but includes the physical aperture limitations. Figure 9C shows the MA, i.e. the off-momentum DA at the septum exit for fixed momentum. Figure 10 shows the local MA along the lattice, as it is relevant for Touschek lifetime (i.e. tracked particles were started on-axis with momentum offset). With 10 pm of vertical emittances and 400 mA in 440 of possible 480 bunches, a Touschek lifetime of 7.2 h is obtained using the simple-Bruck model, or 7.0 h using the more detailed Piwinski-model. Assuming 10⁻⁹ mbar of carbon monoxide as residual gas, as expected after a beam dose of 100 Ah, and including the reduced undulator apertures results in Coloumb scattering and bremsstrahlung lifetimes of 35 h and ~90 h respectively. With bunch lengthening by about a factor three due to the 3rd harmonic cavity, a total beam lifetime of 11.5 h for the ideal lattice is expected (without insertion devices). Intra-beam scattering blow-up is not included.

Performance figures for DA, MA and beam lifetime for the real lattice including coupling and imperfections will be given in section 'real lattice performance' below.

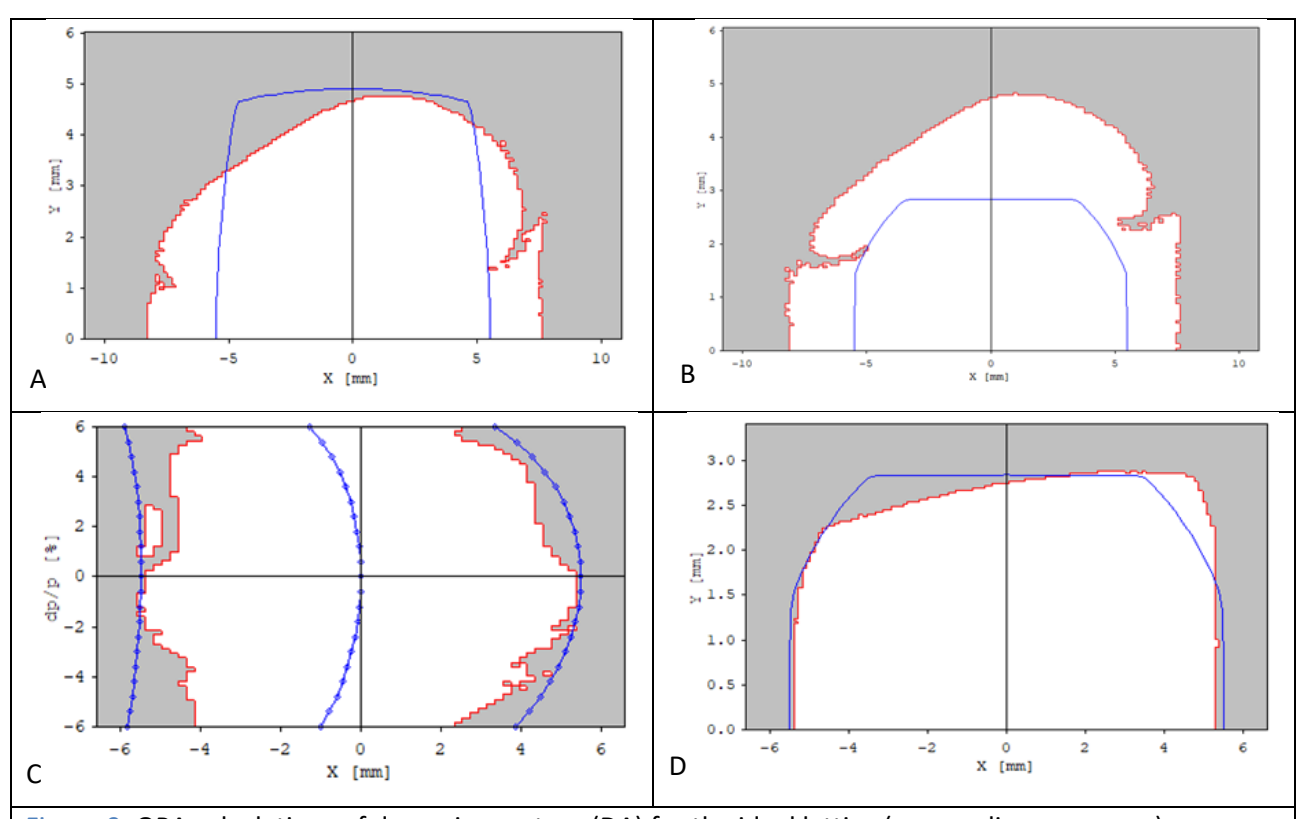


Figure 9: OPA calculations of dynamic aperture (DA) for the ideal lattice (no coupling, no errors).

A) without and B) with insertion devices. The blue contours show the linear projection of all apertures to the trackpoint, which is at the exit of the thin septum, where the beta functions are 23 m / 5.9 m (dotted line in Figure 7). The regular beam pipe of 18 mm inner diameter was assumed everywhere, except at the superbends with 10 mm full inner height and the injection septum was assumed to be located at x = -5.5 mm with its inner edge. C) shows the momentum acceptance, i.e. off-momentum horizontal DA at the septum exit, calculated for fixed momentum. D) is the same situation as B), i.e. DA with insertion devices, but now including the physical aperture limits in the tracking. (Note, that DA locally exceeds the aperture projections due to separate horizontal and vertical loss checks which implicitly assumes rectangular beam pipes, whereas the projection is calculated for elliptic apertures).

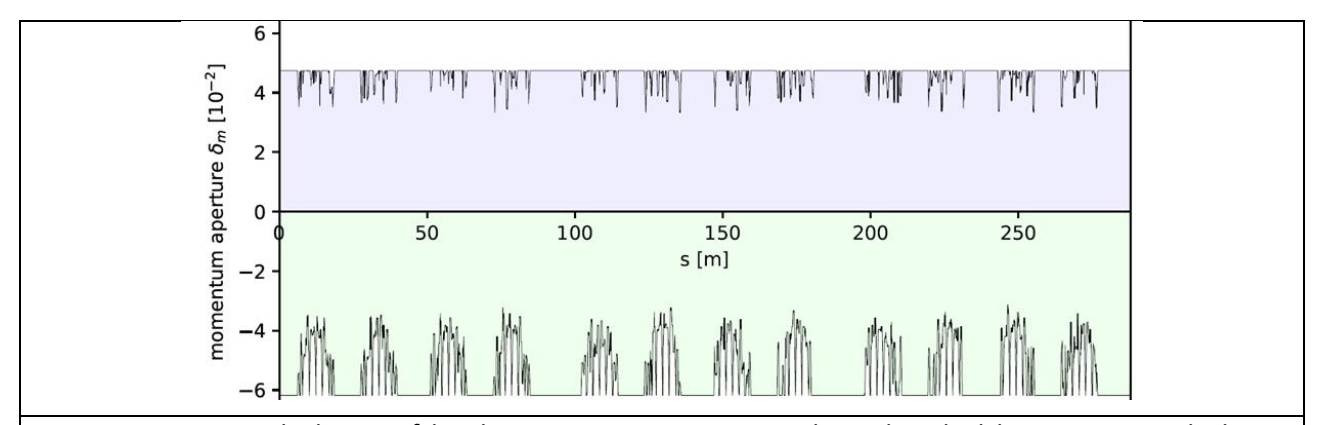


Figure 10: TRACY calculation of local momentum acceptance along the ideal lattice. A 6D-calculation including synchrotron oscillation and damping gives slightly larger RF-MA (c.f. Figure 8), since particles kicked to positive momentum slightly beyond the separatrix are captured due to radiation.

Tuning range and correction capability

The parameters in Table 1 and the optical functions shown in Figures 1 and 3 to 7 refer to the nominal optics at the working point {39.37, 15.22}, which was optimized with respect to brightness and non-linear dynamics. However, some tuning range has to be provided to move the working point around to some extent in order to empirically avoid harmful resonances, or to try modified optics modes for improved brightness or lifetime. On the other hand, lattice imperfections, in particular misalignments, lead to orbit distortions, focusing errors and betatron coupling and need a sufficient number of corrector magnets for compensation. Furthermore, gap-dependent focusing of undulators violates the lattice periodicity and needs to be compensated. In this section the implications for the various magnet types are summarized.

Dipole correctors (CH, CV)

The specifications of dipole corrector magnets, 600 μ rad horizontal (CH) and 400 μ rad vertical (CV), are determined based on estimates for magnet imperfections, misalignments and feedback requirements. The horizontal corrector is stronger than the vertical one with an additional pair of coils connected. This is to compensate for possible deviations (imperfection) of the lattice bending fields in addition to misalignments. Once beam is successfully stored, the required corrector strength can be reduced by realigning bending magnets, and the additional coils can be disconnected in order to align corrector resolutions in the horizontal and vertical plane. It goes without saying that the functionality of the correctors is closed-orbit correction. The magnets together with power supplies will have sufficient bandwidth and resolution to apply orbit corrections within a fast feedback loop. Static and fast orbit corrections are performed with the same system, which motivated the small corrector strength of 400 μ rad in the first place.

A system for remote girder alignment will be implemented (see the chapter on mechanical engineering for details) to interactively correct vertical position and roll with stored beam, as successfully applied at SLS [1.09]. The so-called "Beam-Assisted Girder Alignment" (BAGA), which is based on the analysis of mechanical survey data, and "Beam-Based Girder Alignment" (BBGA), which uses solely beam data for the girder adjustment, perform three tasks: 1. Free vertical corrector strength for steering photon beams following user requests. 2. Correct ground settlements. 3. BBGA and BBGA efficiently suppress spurious vertical dispersion, which is mainly generated by vertical steps between girders, and betatron coupling, which is mainly introduced by vertical beam offsets in sextupoles and roll errors of quadrupoles, in order to provide a largely uncoupled lattice without powering skew quadrupoles. On this base the vertical dispersion wave is deliberately built up to generate the required vertical emittance without introducing betatron coupling in the straight sections.

Main quadrupoles (QP, QPH)

Large scale variations of the ring tunes are performed using the quadrupoles in the matching sections, under the constraints that a) all straights have same phase advances, b) the optical functions inside the arc are not changed, and c) the gradients of the quadrupoles in the straights don't exceed the maximum values of 93 T/m for the QP type and 98 T/m for the QPH type (Table 10). Then the tuning procedures as described in sec. 1.3 are applied to all straights. In this way the working point can be moved within the tune region $[39.0, 40.0] \times [15.0, 15.7]$. At nominal $Q_y = 15.22$, a horizontal range [38.0, 40.6] is accessible. Vertical tune $Q_y < 15$ can only be reached if some beating of the vertical beta function in the arcs is tolerated. However, only the nominal working point has been optimized with regard to non-linear dynamics, and only its vicinity is seriously considered for operation.

Additional gradient increments for compensation of individual undulator focusing may reduce slightly the tuning range, however these increments are relatively small (<3 T/m).

Tuning quadrupoles (QA)

The octupoles in the SOQ magnets contain a total of 264 individually powered tuning quadrupoles, which perform several tasks:

- Correction of gradient errors due to imperfections/tolerances of the VB and AN magnets.
- Compensation of VB, AN gradients due to cross talk when varying the currents of adjacent sextupoles.
- Correction of beta-beat due to misalignments.
- Matching of arc optics to superbends (Figure 3).
- Perform beam based alignment (BBA).

Within the maximum gradient range (± 5.6 T/m, Table 10) the QAs are able to compensate a maximum gradient error of either 2.2% in VB or 1.2% in AN, if no other task is requested. Alternatively, the QAs can be used to shift the unit cell tunes and with it, the ring tunes within a diamond shaped range of approximately $\pm 0.9 \times \pm 0.7$, in principle.

The BBA procedure calibrates the positions of BPMs near the QA and centers the beam in the SOQ, which is achieved by a rigid mount of the octupole containing the QA relative to sextupole inside the SOQ magnet.

Skew quadrupoles (QS)

The octupoles in the SOQ magnets also contain a total of 264 individually powered skew quadrupoles (QS), which are used to set and correct betatron coupling and vertical dispersion, and to adjust the vertical emittance to a moderate value compromising beam life time and brightness. Vertical emittance is created by closed bumps of vertical dispersion inside the arcs while linear coupling (betatron coupling) is largely suppressed in order to a) avoid tilted beams at the source points and b) to prevent the horizontal oscillations of Touschek scattered particles from coupling to the vertical in order to avoid losses at small undulator gaps. For a total beam lifetime of about 10 hours as in the existing SLS, a vertical emittance of about 10 pm is required. Creating this emittance by vertical dispersion bumps and further including lattice imperfections and coupling suppression, a maximum strength of 3.8 T/m was found for the QS, which led to the gradient specification of ±5.6 T/m for 50 mm magnetic length (Table 10). For more details see section 'real lattice performance' below.

Sextupoles (SX, SXQ)

The chromaticity is adjusted by sextupoles in the arc to small positive values in both planes. Damping of coupled bunch instabilities however may require somewhat larger chromaticity and with it more sextupole strength. For non-linear optimization, so-called harmonic sextupoles are added in the matching sections to complete the arc cancellation pattern, and the 288 sextupoles are grouped in nine families to cancel out their adverse effects, which results in some families exceeding the strength required for chromaticity adjustment. The maximum strength $B''/2 = 5850 \text{ T/m}^2$ for 9 cm magnetic length covers all situations encountered in the optimization.

Off-momentum, the 12-fold symmetry of non-linear optics is violated to some amount, since quadrupoles in straights contribute to off-momentum terms too. In addition, compensation of individual undulator focusing, as well as imperfections of the lattice, break the symmetry and may excite non-systematic resonances. As demonstrated at the existing SLS [1.04], deliberate symmetry breaking of the sextupole pattern can suppress non-systematic resonances. The grouping of sextupoles in SLS2.0 (i.e. the connection to power supplies, where each one feeds several units) was optimized to provide maximum flexibility for this non-linear correction [1.05]. A sextupole power supply can drive up to 6 magnets in series. The 264 sextupoles in the SOQs are thus connected in 32 circuits of 6 and 18 circuits of 4 accordingly. The 24 SXQ standalone large aperture sextupoles are grouped in 12 circuits of only 2, since they need higher voltage.

Octupoles (OC)

264 octupoles (OC) in the SOQ magnets are employed to perform 1^{st} -order correction of 2^{nd} -order sextupole effects like ADTS and 2^{nd} order chromaticity. Here a specification of B'''/6 = 63'000 T/m3 for 5 cm magnetic length is determined from dynamic aperture optimization. The octupoles have individual power supplies. This was not a beam dynamics requirement but emerged from the design of the (air-cooled) magnet and of course helps to suppress non-systematic octupolar resonances.

Magnet specifications

Lengths and spaces

Since the lattice is highly compact and the 7-MBA lattice requires rather strong magnets, the approximated magnet parameters were determined by beam dynamics and magnet experts together at the early stage of lattice design. Especially the total length and the space between components were important aspects in order to come up with a feasible lattice solution from the engineering (or integration) point of view. These numbers have been adjusted through iterations, but not changed drastically during the lattice design.

Table 6 summarizes the fixed total length of components used as building blocks for the lattice, and Table 7 displays a matrix of minimum distances between components preserved for mounting.

At the same time, it was concluded that all bending magnets (except for the high field superbends with superconducting coils) should be permanent magnets since the longitudinal space required for the coils of electromagnets was not affordable.

Table 6: Total lengths of components

Component	Length (mm)
BNV compound bending magnet, or superbend with adjacent VB magnets	775.0
BE dispersion suppressor end bending magnet	242.5
VE dispersion suppressor combined function magnet	240.0
AN reverse bending magnet	140.0
ANM reverse bending magnet in dispersion suppressor	150.0
QP small quadrupole	170.0
QPH large quadrupole	210.0
QA-SLS old SLS quadrupole to be re-used in 1L	340.0
SOQ compound magnet: sextupole and [octupole with quad and skew quad coils]	230.0
SXQ standalone sextupole magnet with quad corrector coil	140.0
CHV BPM horizontal/vertical corrector and beam position monitor unit	130.0
CHV BPM-SLS large aperture corr/BPM unit for injection straight [WIP]	170.0

Table 7: Distances between components (with total lengths from Table 6), all in units of mm. (-/- means that this combination does not occur).

to entry \rightarrow	Bends	Reverse	Quad	SOQ	SXQ	Corr/BPM
distance exit ↓		Bends				unit
Bends BNV, BE, VE	-/-	-/-	-/-	30	10	-/-
Reverse bends AN, ANM	-/-	-/-	-/-	10	-/-	22.5
Quadrupole QP, QPH, QA-SLS	-/-	-/-	-/-	10	-/-	22.5
SOQ magnet SOQ	30	10	10	-/-	-/-	-/-
Sextupole SXQ	10	-/-	-/-	-/-	-/-	-/-
Corrector/Monitor [BPM CHV]	47.5	-/-	17.5	17.5	-/-	-/-

Magnet specifications from beam dynamics

Magnets are described in detail in another chapter of this TDR. Here we introduce the names and properties as they were used like "LEGO blocks" for the idealized lattice model. Within this scope all magnets have either cylindrical or Cartesian symmetry, i.e. the beam orbit coincides with a magnetic equipotential, and zero length fringe fields (hard edge approximation). Realistic magnet design and modeling, including bending in straight magnets, finite fringe fields, systematic multipole errors and crosstalk between adjacent magnets, leads to (minor) modifications of parameters. These effects are most important for the permanent magnets, where tuning capabilities are limited.

Parameters are given for a beam momentum of exactly 2.700 GeV/c, then the magnetic rigidity, which translates fields, gradients etc. to curvature, focusing strength etc. is given by

$$(B\rho) = p/q = -p/e = -pc[eV]/c = -9.00623 \text{ Tm}.$$

Table 8 lists the specifications of pure dipole magnets, and Table 9 the combined function magnets, which are basically horizontally displaced quadrupoles, and Table 10 the electromagnets.

Explanations

- "Length" is length as used in beam dynamics with hard edge approximation. It does not correspond exactly to the iron length or the effective field length.
- Total length includes coils etc. and is space reserved for magnets in the lattice keeping the distances and total lengths from Tables 6-7.
- Several magnets exist in two mirror image types; this is indicated by suffix I/O for incoming/outgoing as seen from the arc.
- In case of V*I/O the yokes are mirror images.
- In case of QP, QPH the yokes are the same for I/O types but since connectors are on the inner side
 of the ring, reversing a magnet requires a mirror image.
- In case of SOQ, also the ordering is reversed, i.e. SOQI = [OC, SX] in beam direction, and SOQO opposite.
- Some SOQs contain sextupoles or octupoles with wider yokes for passing the photon beams, which is indicated by "W" (wide) or "WS" (special wide). SOQDO contains a sextupole with retracted coils and increased yoke size to allow visible light to be extracted from the first dipole in the arc (beam lines X**DD).

Table 8: Specifications of pure dipole magnets (PM = permanent, SC = superconductive, LGB = longitudinal gradient bend).

Name		BN	BS2	BS5	BEI	BEO
Туре		PM hom.	PM LGB	SC tunable LGB	PM	
Length	mm	405	405	405	242.500	
Peak field	Т	-1.35066	-2.099	-3.045.42	-1.141	
Angle	deg	3.480	3.480	3.480	1.760	
edge in	deg	1.740	1.740	1.740	1.76	0.0
edge out	deg	1.740	1.740	1.740	0.0	1.76
Number		56	2 [4]	2 [0]	12	12

Table 9: Combined function magnets (all PM)

Name		ANI	ANMI	VB	VBX	VEI
Ivallie		ANO	ANMO	VD	VDA	VEO
Length	mm	140.000	150.000	185	.000	240.000
Field	Т	+0.26947	+0.27246	-0.84	1967	-0.65495
Gradient	T/m	-77.6562	-82.8733	+40.6704	+33.1328	+45.7648
Angle	deg	-0.24	-0.26	1.000		1.000
Edge in	deg	-0.24	-0.26	0.5	0.5	1.0
	ueg	0.0	0.0	0.5	0.5	0.0
Edge out	deg	0.0	0.0	0.5	0.5	0.0
Luge Out	ueg	-0.24	-0.26	0.5	0.5	1.0
Number		60	12	96	24	12
Number		60	12	50	24	12

Table 10: Electromagnets

Name		QP	QPH	QA	SOQ		SXQ	CH	V
		[-I/O]	[-I/O]	(SLS)	[-I/O/WI/W0	D/WSI/DO]			
L _{total}	mm	170	210	340	23	0	140	10	5
					SX	OC	SX	СН	CV
Length	mm	100	140	200	90	50	90	< 0 >	< 0 >
$\int B_y / B_x dI$	mTm	-/-	-/-	-/-	-/-	-/-	-/-	3.6(+1.8)	3.6
B'y/ B'x	T/m	93/0	98/0	23.2	-/-	5.6/5.6	-/-	-	
B" _y /2	T/m ²	-	-	-	5850	-	5850	-	
B" _y /6	T/m ³	-	-	-	-	63000	-	-	
Numbers		55	53	4	264		24	113	2
		[31/24]	[29/24]		[72/96/24/	24/36/12]			

The magnets VB* are rectangular magnets with edge angles of 0.5° on both sides, however, they are very close to the BN magnets to form the [VB,BN,VB] = BNV triplet, so the field will not drop in the small gap between.

- BS2 is a permanent magnet superbend. Four of these will be installed in "Phase 1". In "Phase 2", two of them will be replaced by the tunable, superconducting superbend BS5. Superbends replace BN magnets and form triplets with two VB*s.
- Internal spaces as assumed in lattice files [mm]:
 - SOQI = 15 (coil) + 50 (OC) + 15 (coil) + 10 + 25 (coil) + 90 (SX) + 25 (coil) = 230
 - CHV = 25 + 0 (CV) + 55 + 0 (CH) + 25 = 105 (correctors as thin kicks)
 - BPM = 25
- Other spaces may be seen from the "Holy List" (the master list of all components which make up the storage ring).

Validation of realistic magnet designs

During lattice design, idealized, 2D multipolar fields of different magnet types, piece-wise constant along the beam path, are assumed. The actual 3D magnet design may deviate due to limits and differences in yoke shape and magnetization, leading to unwanted higher-order multipoles and deviation from the desired multipoles inside the magnet, as well as fringe effects and cross-talk effects on the magnet edges.

To study these effects, volumetric maps of the magnetic flux density are analysed in a validation loop between the magnet group and beam dynamics, thus iterating the initial magnet designs until all requirements are met.

The validation is performed by fitting the multipolar fields (polynomial expansion including fringe effects) in steps of 1 mm around the trajectory to the values, the multipoles are generalized to also include fringe effects. When importing these multipole slices into the lattice simulation, their behavior on beam dynamics (tune footprint and dynamic aperture) is analyzed.

At the time of writing, the iterations on the BN-VB magnet are almost complete, and work is in progress for the other magnets.

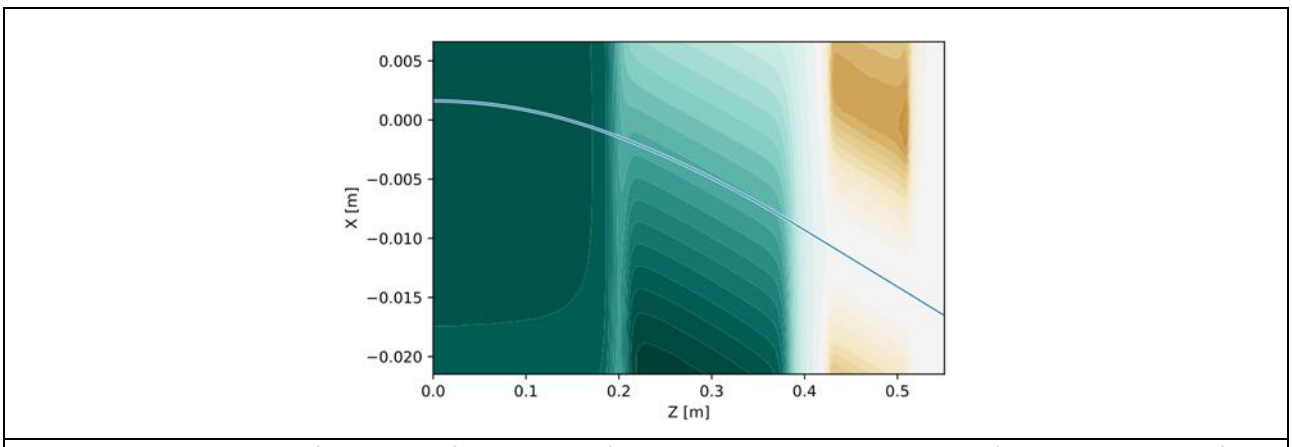


Figure 11: Distribution of magnetic field density (green positive, orange negative) in a simulation of the BN-VB combined function magnet with attached sextupole (Opera model: M. Negrazus). The trajectory shown in blue yields the desired bending angle of 2.74° without active sextupole magnet.

Injection concept

The injection should be compatible with the limited machine aperture. At the location of the injection septum, where the horizontal beta function is increased to be about 23 m, the dynamic aperture with machine imperfections will be at least 5 mm, which is three or four times smaller than that of the SLS. The injection into such a small aperture is a common challenge for the next generation light source.

Two injection schemes are proposed and to be implemented:

- 1) Conventional kicker-bump injection as in the SLS
- 2) "Aperture sharing" using a short pulse kicker

The available aperture is quite limited as discussed, and thus it is not straightforward to apply the conventional injection. To this end, two important parameters, namely the injection beam emittance and the septum blade thickness, are improved. The injection beam emittance can be lowered through an emittance exchange in the booster, and it has been experimentally proved [1.06]. The septum blade can be 1-mm thick by dividing the injection septum into thick and thin ones as in the ALS [1.07]. These improvements make it possible to apply the conventional injection scheme together with the high beta function at the location of the septum.

The quadrupoles, BPMs and correctors in the straight section of Sector 1 need to be large aperture ones. These components are included in Tables 6, 7 and 10.

The second injection scheme, "aperture sharing", is based on a short pulse kicker, which is to be installed in the straight section of Sector 2, downstream of Sector 1 straight section, where the injection septa and the kicker bump are installed. The injected beam goes through the first arc with large betatron oscillation amplitude and is inflected within the aperture by the short pulse kicker. The stored beam bunches are also deflected by the kicker. However, they stay within the aperture when the deflection is small enough. Thanks to the thin septum, this condition can be fulfilled. The number of bunches to be disturbed by the kicker depends on its pulse length. A kicker pulse of 20 ns level is feasible with the present technology, limiting the number of disturbed bunches to 10 out of 460 stored. The pulse can be shortened to the nanosecond regime in the future, realizing a quasi-transparent injection. Aperture sharing benefits the smaller injection beam emittance and the thin septum as well.

The residual betatron oscillation at the septum is <4 mm with these injection schemes. Since the horizontal beta function at the locations of the insertion devices are much smaller, the oscillation is minimised there. Therefore, the injection is compatible with not only the dynamic aperture but also a circular aperture radius as small as 4 mm at the insertion device locations (Apple type undulator).

The specifications of the injection elements are listed in Table 11. The kicker bump of the present SLS is compatible with the injection into SLS2.0 storage ring, and thus it may be re-used. The short pulse kicker is divided into two: one is installed in the first part of Sector 2 straight section and the other in the last part, leaving room for an undulator in between. This configuration removes the constraint on the phase advance between the septum and the short pulse kicker, which should otherwise be a multiple of 90 degrees.

The details of injection, including tracking simulations, are found in [1.08].

Table 11: Design specifications for injection elements. The total length is reserved length as the ones for the magnet (Table 6). Technical specifications include some reserve (c.f. chapter on injection hardware).

	Total length	Deflection angle	
Thick septum	1.90 m	7°	
Thin septum	0.71 m	13.5 mrad	
Short pulse kicker	2×0.8 m	~300 µrad each	
Kicker bump	4×0.85 m	<3 mrad each	

Real lattice performance

Error scenario and correction

Alignment errors are applied to girders (60 μ m RMS), girder joints (20 μ m RMS) and elements on girders (30 μ m RMS), (Table 13). The Gaussian distributed errors are confined to an interval of ± 2 sigma reflecting the expected initial alignment errors. BPMs are assumed to be correlated to adjacent sextupoles within 5 μ m RMS. This corresponds to the expected cumulated Beam-Based Alignment error with respect to the adjacent tuning quadrupoles (QA) realized as additional coils in the octupoles (OC) and their known offsets with respect to the adjacent sextupoles (SX) inside the SOQ compound magnet.

The SVD based orbit correction utilizes 126 BPMs and 114 horizontal and vertical correctors without eigenvalue cut. Correctors are assumed to have a resolution of 18 bits or 4 ppm in amplitude. The optics is corrected using the 264 tuning quadrupoles (QA). Beta function measurements can be done by either using LOCO techniques or modulating the tuning quadrupoles as done in the simulation. Beta beats of <1% are achieved in both planes.

Consecutively 264 skew quadrupoles (QS) are used to correct the betatron and emittance coupling. The vertical dispersion is corrected to a predefined dispersion pattern with vanishing dispersion in the straights. The emittance coupling is deliberately increased to 6.6% while the betatron coupling is simultaneously suppressed to <0.1%. The coupling correction is followed by another iteration of beta beat correction. The design tunes are kept constant during the correction process by using the tuning quadrupoles.

Smooth tuning

Besides the methods for lattice tuning described in section 1.7 a smooth small-scale tuning is applied to the lattice by setting all quadrupoles; the 112 main quadrupoles as well as the 264 tuning quadrupoles. This is routinely applied to the existing SLS in operation to empirically improve injection efficiency and beam lifetime, and works well, i.e. perturbs the periodicity negligibly, if the tune shifts are small, say <0.1. A similar interactive tuning method will be enabled at SLS2.0 by the dispersion free octupoles in the matching sections to manipulate the ADTS and tailor the tune footprint.

In tracking studies it turned out, that on-momentum dynamic aperture becomes more robust to imperfections if the working point is shifted slightly from $\{39.37, 15.22\}$ to $\{39.39, 15.22\}$ to keep more distance to the non-systematic 3Qx = 118 resonance. Alternatively, the resonance could be suppressed deliberately as described in Sec. 1.7/Sextupoles. This could as well be a result of "trial & error" in the control room. Results shown in this section are for the shifted working point.

Dynamic aperture

Figure 12 shows the dynamic aperture with and without the vertical dispersion bumps for generating 10 pm of vertical emittance, with and without systematic multipole errors as obtained from 3D magnet simulations and the results of 12 seeds of random misalignment after correction. In all cases, the dynamic aperture is larger than the physical aperture (Figure 9A/B) and thus predicts full capture of the injected beam.

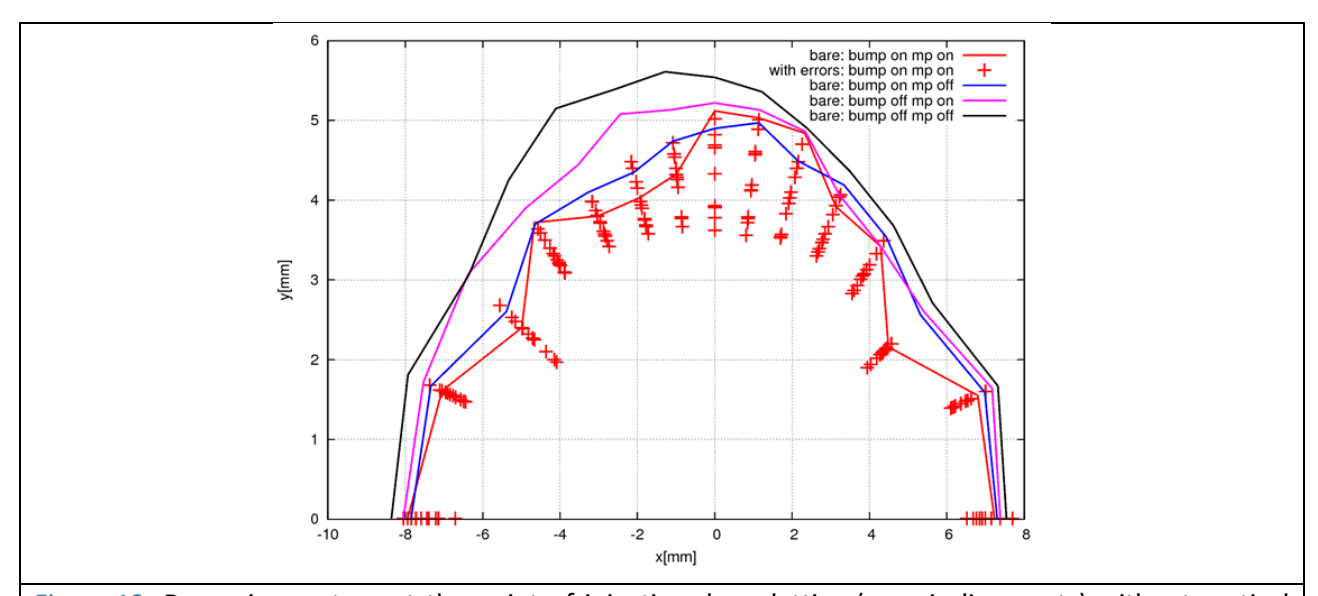


Figure 12: Dynamic aperture at the point of injection: bare lattice (no misalignments) without vertical dispersion bump in black (compare to Figure 9A), with dispersion bump in blue, with systematic multipole errors in magnets and no dispersion bump in pink, and with dispersion bump in red. The red crosses are the results for 12 seeds of corrected misalignment errors. Beta functions at track point are 23.0/5.9 m.

Beam lifetime

Figure 13 shows Touschek lifetime results for the lattice including vertical dispersion bumps, without and with 12 seeds with imperfections and corrections. Lifetime was calculated in the classical, one-dimensional by Bruck [bruck], and in the relativistic model including coupling by Piwinski [piwi], which usually gives about 10% lower results. Without the 3rd harmonic cavity and assuming 400 mA in 450 bunches a lifetime (Piwinski) of 6.0 h is obtained for the error-free lattice, and an average of 5.1 h for the 12 seeds, with 3.4 h for the worst seed. These values would be tripled approximately by a 3rd harmonic cavity. Taking into account 35 h Coloumb scattering lifetime and about 90 h bremsstrahlung lifetime (section 'non-linear optics'), an average beam lifetime of 9½ h is expected, and still 7¼ h for the worst seed.

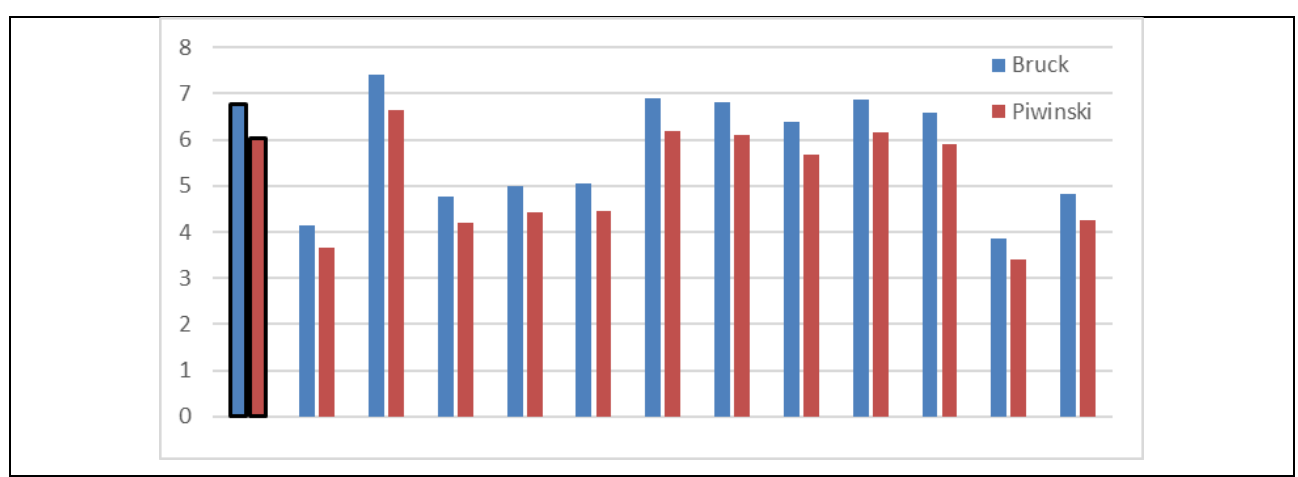


Figure 13: Touschek lifetime results for 12 seeds of the lattice with dispersion bump and corrected misalignment, calculations based on the models by Bruck and Piwinski. The first point is for the lattice without errors. An emittance of 10 pm and no harmonic RF was assumed.

Frequency maps

Figure 14 shows frequency maps, i.e. the diffusion rate of the tunes, to visualize the active resonances. The figure shows the lattice without imperfections but including the vertical dispersion bumps. On-momentum DA is large and robust, the ADTS are well controlled, and the footprint is confined to a small area in tune space. The MA shows some degradation at the negative momentum side due to the Qx + 2Qy = 70 coupling resonance, which is not systematic but off-momentum, the 12-fold periodicity is violated. Touschek scattered particles reach amplitudes up to x $\boxed{2}$ 5 mm for $\delta p/p=\pm5\%$, so they can get lost in this region, which probably is responsible for the reduced lifetime found for some random seeds of imperfections. Certainly, there is room for further improvement. Nevertheless, even the worst-case lifetime is sufficient, and further means for tuning, like shaping the footprint using octupoles, have not yet been applied.

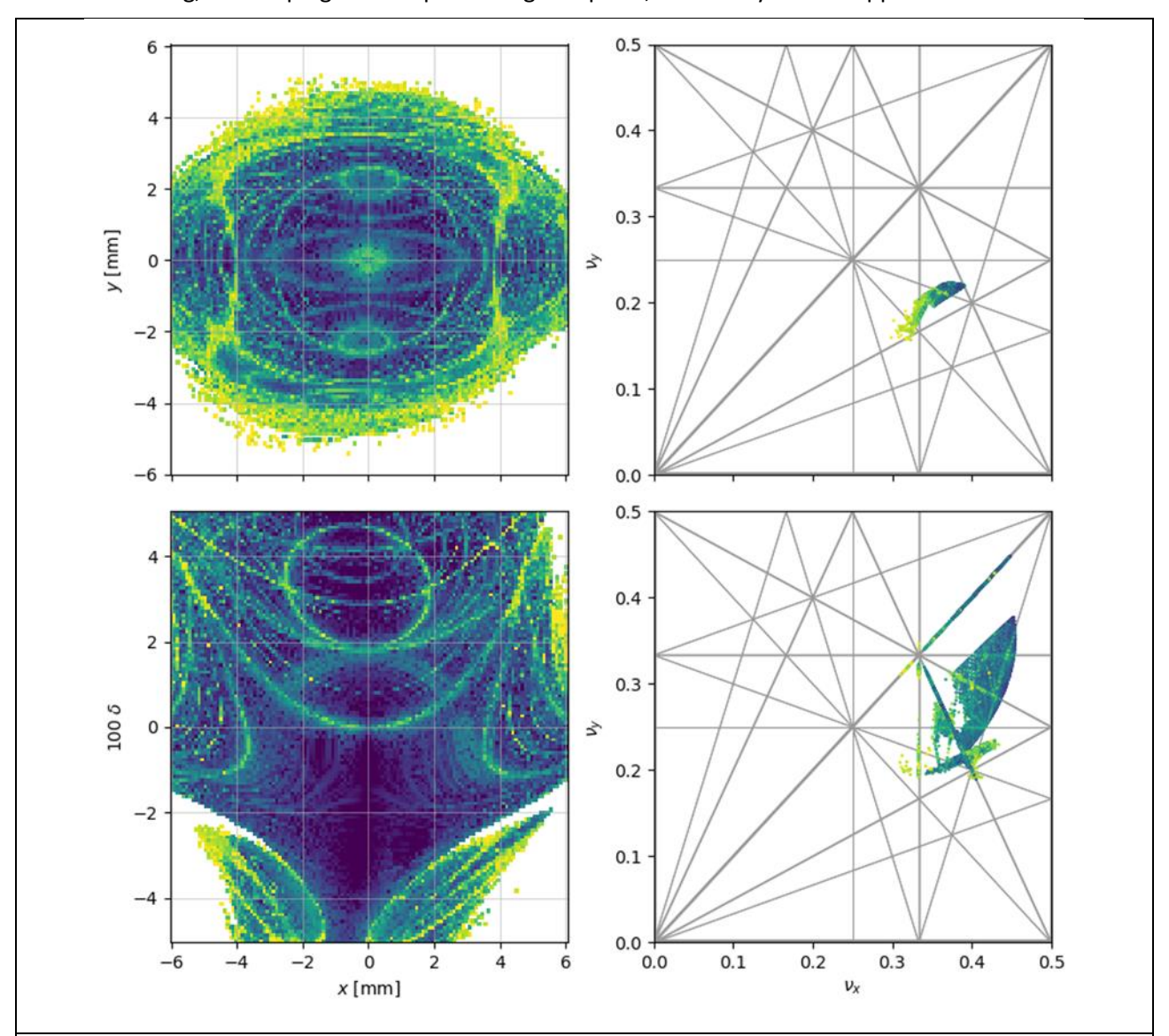


Figure 14: Frequency maps in transverse space (x,y), (top left) and in momentum space (x, $\delta = \Delta p/p$) (bottom left), and in tune space (right side) for the error-free lattice including the vertical dispersion bumps. The stable region in the top left figure corresponds to the blue curve in Figure 12.

Impact of insertion devices

The focusing effect from undulators is compensated with the procedures described in 'straight sections' for matching to the straight sections: four quadrupole pairs in the short straights restore tunes and symmetry, and ≥6 quadrupoles in the other straights restore tunes and periodic continuation. In the short straights, this implies a perturbation of periodicity-12 of nonlinear optics, since sextupoles and octupoles are located between the quadrupoles, but the undulator focusing is rather weak, so the impact on dynamic apertures is tolerable (Figure 9B vs. A). However, the undulators contain static and dynamic multipoles due to field roll-off and other imperfections. As a first test case, the elliptical undulator UE36 (Table 3) is investigated based on a 3D-field map provided by ID design. As a first step, the residual field integral is compensated by an artificial kick of 8 µrad, equivalent to a local corrector. Using the corrected trajectory as a reference, multipoles are calculated from a polynomial fit applied to the vertical component of the field on segments perpendicular to the reference trajectory. Figure 15 shows the multipoles thus obtained along the undulator UE36. Typically, in planar undulators the integrals of the even terms (dipole, sextupole) cancel in each full period. Figure 16 shows the dynamic aperture without and with 3 × 2 UE36 undulators in the medium straights and demonstrates that the impact on dynamic aperture is well tolerable. Work is in progress for the other undulators also.

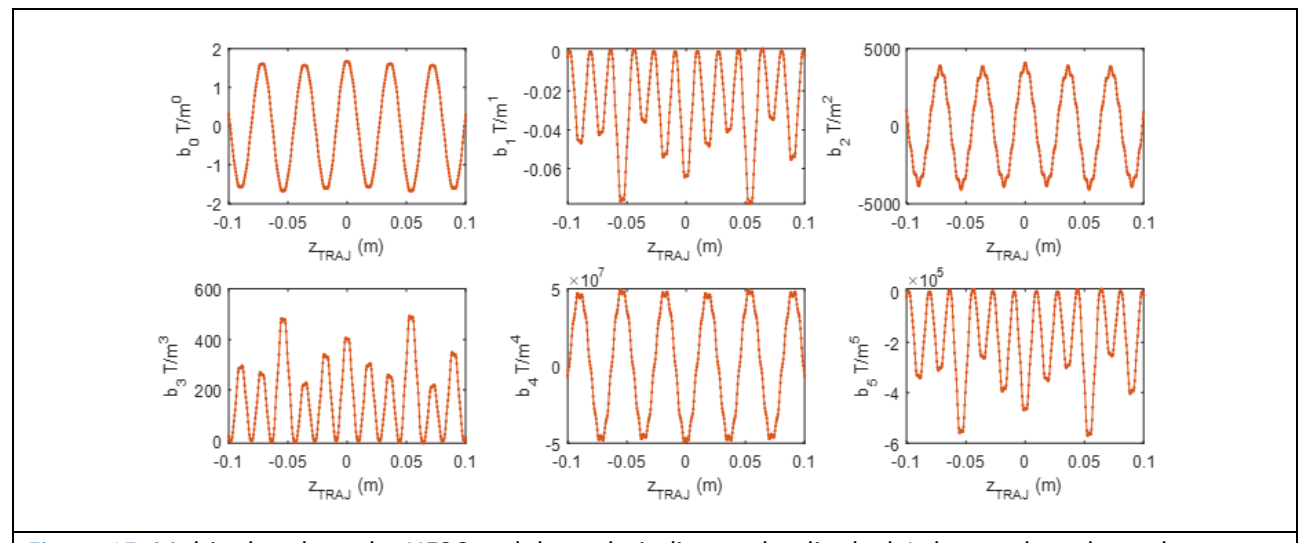


Figure 15: Multipoles along the UE36 undulator. b₀ indicates the dipole, b1 the quadrupole, and so on.

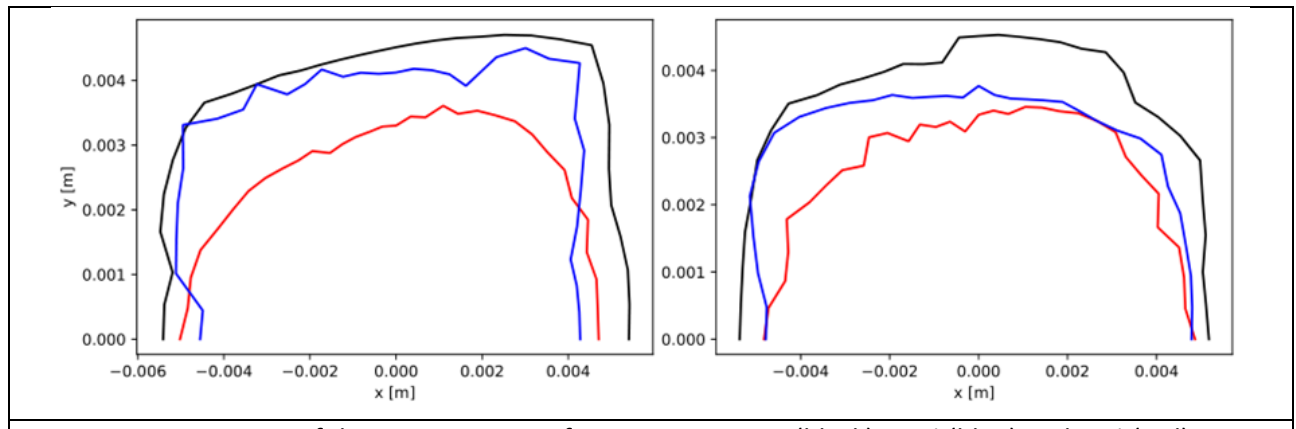


Figure 16: comparison of dynamic apertures for on-momentum (black), +3% (blue) and -3% (red) energy deviation for ideal lattice (left) and with UE36 multipole insertions (right). Aperture limitations from UE36 and from the injection septum were included here (Figure 9D).

Booster to ring transfer line (BRTL)

The new geometric layout of the SLS 2.0 storage ring injection requires a modification of the booster-to-ring transfer line (BRTL), which will also include extended diagnostics capabilities for determination of beam properties from the booster to allow thorough control and optimization of injected beam parameters.

A technical note [1.10] describes the upgrade in more detail and the element line-up is given in [1.11]. The main feature of the new BRTL is an achromatic region to disentangle emittance and energy spread measurements. Tomographic phase space measurements can be done at the location of the screen monitor SM-2 in both transverse planes by varying the strength of the QB1...4 quadrupoles, providing sufficient tune ranges of > 170° of the horizontal and vertical betatron phase. Optics settings, quadrupole strengths, beta functions at the measurement screen SM-2 and tune advance from the start point to SM-2 can be taken from [1.10]. Energy spread can be measured at the location of the screen monitor SM-4. By switching off the QC1...4 quadrupoles, the dispersion is determined only by the (well-known) dipole angles (B-2 and B-3). The betatron contribution to the beam size at SM-4 is low, such that the energy spread of the extracted beam from the booster can be measured with <1 % resolution (assuming 20 µm spatial resolution of SM-4). The re-use of quadrupoles and bending magnets from the present SLS BRTL [1.12], the integration of additional quadrupoles and combined screen / beam position monitors from the SwissFEL Injector Test Facility (SITF) as well as the utilization of power supplies from the discarded SLS electromagnetic undulator X09LA-ID will result in only moderate investments for supports and vacuum chambers for the upgraded SLS2.0 BRTL.

Figure 17 shows the schematic layout and the nominal optical functions of the new BRTL for injection into the SLS2.0 storage ring. The booster extraction septum and the thick storage ring injection septum are both considered parts of the SLS2.0 BRTL, since they only affect the extracted / injected beam but not the circulating / stored beams. For the "kicked beam" at the top of the booster ramp, the BRTL starts at the exit of the booster dipole ABOMA-BD-6E in front of the extraction septum ABOMA-YEX, assuming that the booster extraction kicker ABOMA-KEX is set to its nominal kick angle of -0.28°. The upgraded BRTL ends at the exit of the thick storage ring injection septum ABRTL MSEP-0950. Table 12 lists the relevant points in the beam dynamics coordinate system, where the origin is at the WSLA building center and the Y-axis points to the middle of storage ring section 1L. Note that the final angle of the new BRTL is non-zero, since quadrupoles and thin septum follow in the storage ring straight 01L. The injected beam offsets at the thick storage ring septum exit is -26.500 mm for the SLS2.0 BRTL as compared to -26.000 mm for the present SLS BRTL. The parallel shift of the 01L injection straight of +67.509 mm in the new storage ring (Table 2) results in a shift of the new BRTL endpoints by $\Delta Y = +67.009$ mm.

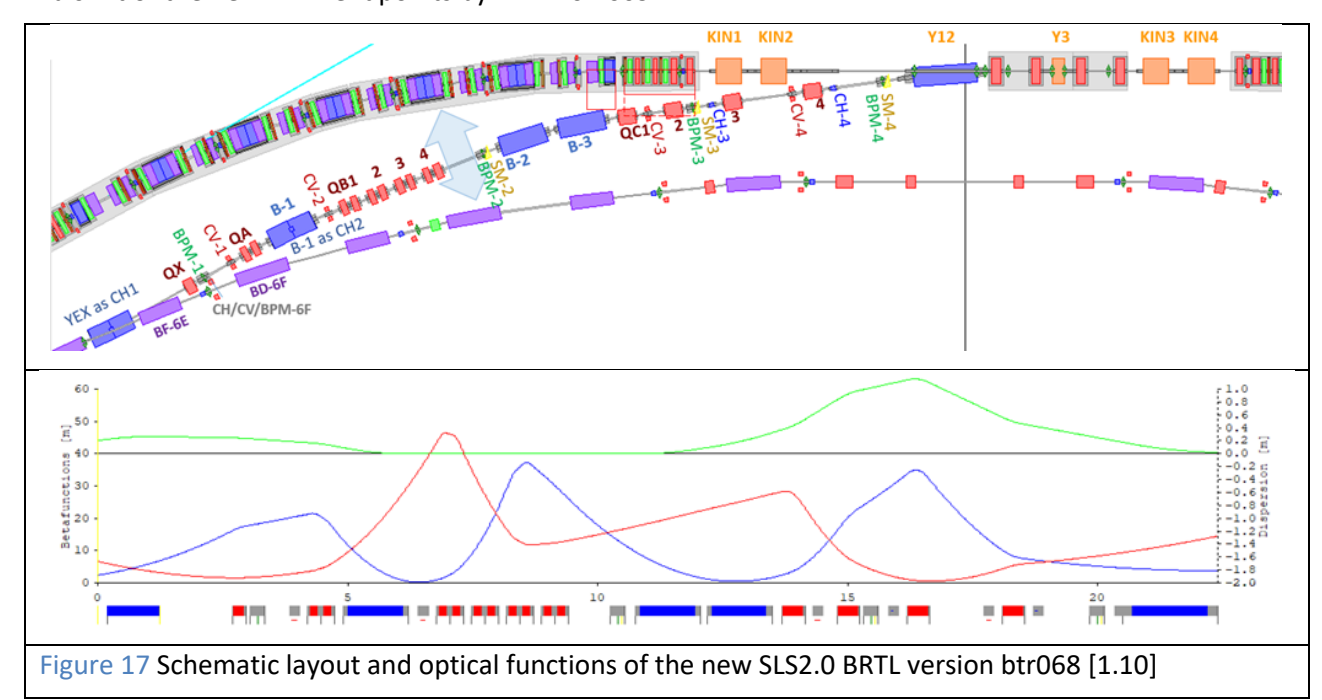


Table 12: old and new transfer line geometry data

Location	X [mm]	Y [mm]	Angle
Start BRTL = kicked beam at ABOMA-BD-6E exit	-20'704.850	37′729.491	23.129′670°
Endpoint existing BRTL (br1opt2cc)	830.000	44'023.237	0.000′000°
Endpoint new BRTL (btr068b)	480.000	44'090.246	1.052′753°

There are three groups of components of the SLS 2.0 BRTL (also see Figure 17):

- 1) Components to be re-used from the existing SLS BRTL. For magnet type data see [1.12]:
 - Three dipoles of type BG including their power supplies. The first dipole B-1 remains at its present location. The dipoles B-2 and B-3 will be operated at a reduced deflection angle from presently 8.200000° (SLS BRTL) to 6.778′249° (SLS2.0 BRTL). This changes the sagitta from 19.7 to 16.2 mm but may still fit in the existing vacuum chambers.
 - One of the QS type quadrupoles (renamed to QX in the upgraded SLS2.0 BRTL) and four of the QL type quadrupoles (renamed as QC-1...4). All but QC-1, which needs more current, may re-use the existing power supplies.
 - Four double-correctors of type CH2, CV2, including their power supplies.
 - The booster extraction septum including its power supply stays in place.
- 2) Components from the SwissFEL Injector Test Facility and SLS to be re-used in the upgraded BRTL:
 - Ten quadrupoles of QFA type from SITF.
 - The QFAs will be connected in pairs with six bipolar (4-quadrant) 150 A power supplies (type 67), which are presently still operated at the X09LA-ID electromagnetic undulator, five of the type 67 power supplies will be used for the QFA pairs and one for the QC-1 quadrupole.
 - Four combined resonant stripline-BPM and optical screen monitor units.
- 3) New components (perhaps partial re-use and / or modification possible):
 - The new SLS2.0 BRTL layout and thus the replacement of existing SLS BRTL components
 requires a number of new vacuum tubes, which are connected to the magnet and diagnostics
 assemblies. Since existing SLS BRTL components and re-used SITF components will be mixed,
 a number of tapers, adapting to the different beam pipe cross-sections will also be needed.
 - The existing SLS BRTL supports were fitted to the original layout (mainly magnet and diagnostics assemblies). Only the detailed mechanical design of the upgraded BRTL will show if existing supports can be re-used or retrofitted and which supports need to be newly designed to conform to the new layout and the space conditions especially at the end of the BRTL, close to the components of arc#12 of the storage ring and the O1L injection straight.
 - The newly developed SLS2.0 BPM electronics will also be used for the re-used SITF 500 MHz resonant stripline BPMs, aiming for 10 μ m rms single bunch position resolution at beam charges >100 pC.
 - The screens and the out-coupling / imaging optics of the screen monitors has to be designed newly (or the existing SITF has to be adapted accordingly) to comply with the spatial resolution requirements of 20 μ m for the emittance measurement (tightest focusing of the beam from the booster may result in <20 μ m rms beam sizes).
 - The present SLS BRTL is equipped with four correctors, which are corrector pairs from the booster, capable of making a maximum deflection angle of 1.4 mrad @ 2.7 GeV. In order to have full flexibility, the newly designed SLS2.0 BRTL should ideally be equipped with eight correctors (four in the horizontal and four in the vertical plane).

- Three options for the BRTL correctors are presently followed:
 - a) Split all four corrector pairs from the present BRTL. It has however still to be verified, if 0.7 mrad maximum deflection angle is sufficient for beam steering in the SLS2.0 BRTL.
 - b) Find at PSI or at other institutes four more correctors with sufficient correction strength and large enough aperture (45 mm).
 - c) Design new correctors for the SLS 2.0 BRTL with sufficient correction strength (1.4 mrad @ 2.7 GeV) when using the existing 5 A power supplies.
- The thick injection septum, see Table 11 and Table 12 in injection hardware chapter.

Commissioning

The time window allocated for the commissioning is six months: three months dedicated to the accelerator and another three months in parallel with beamline commissioning. To meet the schedule, the commissioning work should be well organized and prepared in terms of both hardware and software. The preparation of hardware includes systems tests, such as magnet polarity checks in the tunnel, preconditionings of RF cavities and vacuum chambers, etc.

The commissioning is divided into seven phases:

- Phase 1 Linac, booster and transfer line commissioning
- Phase 2 First turn in storage ring
- Phase 3 Second turn and multi turn
- Phase 4 Accumulation, basic feedbacks and linear optics
- Phase 5 Nominal beam current with advanced settings and feedbacks
- Phase 6 Insertion device and collimator setup, making first photon beams
- Phase 7 Finalization

A more detailed commissioning plan is found in a separate document [1.13], which includes also simulation studies referred in this chapter. It has been shown that the storage ring has an error correction capability to achieve the required performance [1.14].

Phase 1 - Linac, Booster and transfer line commissioning

A restart of the linac, which is in a separate tunnel, is foreseen before the main tunnel is closed. Hence it is not included in the time estimation of the beam commissioning.

The SLS booster currently provides the storage ring with 2.4 GeV beams. The beam energy will be increased to 2.7 GeV for SLS2.0. The transfer line from the booster to the storage ring will be newly refurbished with additional quadrupole magnets and beam diagnostic capability.

The emittance exchange in the booster [1.06] needs to be re-implemented during the booster commissioning. Characterization of the booster optics using the refurbished BPM diagnostics, orbit correction and optimization of the ramp is a prerequisite of this procedure. Tests are needed in varying the extraction timing and/or the maximum magnetic field at the flat top such that the extracted beam energy can be adjusted in phase 1.

When booster commissioning is complete, the transfer line optics needs to be properly set up such that the position and angle of the beam at the storage ring injection septum are under control for later injection tuning. The new transfer line is designed to have a non-dispersive section to ease characterization of the extracted beam. The vertical collimator in the transfer line will be set up once the optics is established. This, together with the storage ring collimators, will prevent an uncontrolled injected beam from damaging the storage ring magnets and insertion devices.

The goal of Phase 1 is to establish stable beam with the design parameters at the storage ring injection septum.

Phase 2 - First turn

As soon as the injector chain and the transfer line are ready, we can move on to the storage ring commissioning. The goal of Phase 2 is to establish full control of the first-turn beam trajectory. The BPMs in turn-by-turn mode are essential beam diagnostics, and they will be tested with beam prior to phase 2. Table 13 summarizes the assumed machine imperfections together with the maximum corrector strength.

Table 13: Machine imperfections assumed and corrector strength

Misalignments	
Girder absolute	60 μm rms
Girder-to-girder	20 μm rms
Individual component	30 μm rms
Component roll error	300 μrad rms
ВРМ	
Electronic offset	300 μm rms
Electronic roll error	10 mrad
Resolution in turn-by-turn mode	50 μm rms
Resolution in orbit mode	50 nm rms
Magnet field error	0.2%
Corretor strength	
Horizontal plane	600 μrad*
Vertical plane	400 μrad

^{*} The horizontal corrector is equipped with an additional winding to increase the maximum strength from 400 μ rad to 600 μ rad during commissioning. It will be disconnected when the machine is properly set up and a strength of 600 μ rad is no longer necessary.

The imperfection of the storage ring is dominated by BPM electronic offsets arising from non-identical electronics, each connected to four button channels, and physical offsets with respect to the adjacent magnets. The latter can be significantly large since we cannot align BPMs, which are incorporated to the vacuum chamber, precisely. These offsets can be subtracted, based on alignment survey data before beam commissioning. It is impossible with the given corrector strengths (and actually not desirable) to fully correct the first-turn trajectory with respect to the BPM center determined by the, up-to-this-point, unknown offset. Therefore, the trajectory is first corrected with only effective correctors, i.e., a pseudo inverse matrix with a moderate eigenvalue cut is used when the corrector strength are computed. This "soft correction" will bring the injected beam to the end of first turn as far as the injection beam is properly guided into the storage ring. The kicker bump is used for this such that BPM readings are zeroed at the first two BPMs in the horizontal plane. If the soft correction does not work well, it is an indication of polarity error(s) in a quadrupole, BPM or corrector. Any wrong polarity will be corrected here if it still exists.

Afterward, we apply a special technique to reduce the BPM offset: we regard the BPM offsets as "another set of correctors" and infer the BPM offsets using again a pseudo inverse matrix with an eigenvalue cut. The rms BPM offset can be reduced approximately by a factor of two by applying a proper cut. After correcting the BPM offsets, it becomes possible to apply a "hard correction", i.e., a simple matrix inversion (no eigenvalue cut). Moreover, the injection beam energy can be also evaluated: the average over the BPM offsets found with this technique is proportional to the injection beam energy deviation if the BPM offset distribution is centered to zero. It is noted that sextupoles and octupoles are turned off during phases 1 (and 2) since they modify significantly the trajectory response to the correctors.

A full control of the first-turn trajectory is established through these procedures, i.e., the offset corrected BPM readings for the first-turn trajectory can be all zeroed with the given corrector strength.

To maximize the efficiency of the work, the final commissioning of the RF system (500 MHz) can be performed in parallel (or perhaps even earlier during the booster commissioning) since the acceleration of beam is negligible for the first-turn trajectory. Other transparent activities such as the commissioning of beam loss monitors can be started already in phase 1. The entire work should be parallelized as much as possible to shorten the commissioning time.

Phase 3 - Second turn and multi turn

The second and multi turns, the goal of Phase 3, will be achieved by equalizing the first and second turn trajectories. The kicker bump will be turned off so as not to deflect the injected beam at the end/beginning of its first/second-turn. Instead, downstream correctors in arcs 1 and 2, which do not disturb the equalizing, are used to put the first-turn beam on-axis. Once the equalizing is achieved, the above correctors are set back, and the kicker bump is turned on again. A multi turn may be achieved as soon as the kicker bump is on. Alternatively, a diagnostic kicker and/or the fast injection kicker may be used to launch the first turn beam. However, the static elements (correctors) would be easier to handle at this early stage of commissioning.

Phase 4 - Accumulation, basic feedbacks and linear optics

The sextupole and octupole magnets will be set to their nominal values, and the RF system turned on. Once the injected beam is captured by the RF bucket, we will attempt to accumulate beam. The beam loss monitor may be useful at this time. The BPMs will be switched to orbit mode and become the most important diagnostics in the following steps.

The commissioning of the passive third harmonic cavity system can start once sufficient beam current is stored. With a stored beam, we establish a procedure of closed orbit correction. The commissioning of various diagnostics such as current transformers and beam size monitors also starts in parallel. The synchrotron radiation scouring of the vacuum chambers begins as soon as there is a stored beam. Vacuum pressure is monitored around the ring, and we start recording the integrated beam current (in the archiver). At this time, temperature sensors installed on the vacuum chamber provide a simple protection of the vacuum system. An orbit interlock provides additional safety.

Commissioning simulation showed that the dynamic aperture is most likely large enough for accumulation after phase 3.

As soon as we have a stored beam, the normal beam dump procedure (with insertion devices open) has to be established. Afterward, the slow orbit feedback and RF frequency feedback can be established. The filling pattern feedback will also be prepared to be ready for the next phase. Precise BPM beam-based alignments, and linear optics measurements and corrections follow. Simulation studies showed that LOCO style optics correction can correct beta-beats below 1% rms. Tune feedback is set up once the linear optic is well corrected.

Phase 5 - Nominal beam current with advanced settings and feedbacks

Towards accumulation of the nominal beam current, we proceed through a few steps. First, the skew quadrupoles have to be adjusted to control the vertical emittance. A vertical remote girder realignment at this stage will allow us to achieve small coupling and spurious vertical dispersion. Coupling correction with skew quadrupoles reduces this further prior to the vertical emittance manipulation. The skew quadrupole setting will be confirmed by measuring the orbit response matrix and the vertical dispersion while a direct confirmation by the beam size monitor, which may take some time to commission, may not be available at this point.

In addition, a re-alignment of the combined function magnets in the tunnel might be necessary in order to lower the horizontal corrector strength. We will also consider a horizontal girder realignment at locations where needed. When the maximum corrector strength is well below 400 @rad the additional windings of the horizontal correctors can be disconnected, maximizing the fast orbit feedback performance.

Second, we perform chromaticity measurement and correction. Measurements will be repeated while adjusting the sextupole power supply current family by family and checking that the changes in

chromaticity are consistent to the optics model. Finally, collimators have to be set approximately to protect permanent magnets using the beam loss monitor together with the beam lifetime measurement.

In addition, we may need to get the bunch-by-bunch feedback working if it is essential to stabilize coupled bunch instabilities at the nominal current. In addition, some time will be required for the conditioning of the RF cavity with beam and for the commissioning of the LLRF-feedbacks with beam. Important parameters, such synchrotron tune and Robinson stability must be examined.

Once we are ready, an accumulation of the nominal current is tested, and full commissioning of the harmonic cavity is performed. With a high current beam, the linear optics correction and BPM beam-based alignment may be repeated and elaborated. Nonlinear optics correction is also foreseen to prolong the beam lifetime as much as possible. First commissioning of the fast orbit feedback is carried out in order to prepare for the characterization and operation of insertion devices.

Phase 6 - Insertion devices and collimators, making first photon beams

The insertion devices will be tested one by one, and storage ring collimators will be more precisely set to protect not only the storage ring permanent magnets but also the insertion devices. The beam loss monitor is used here as well. Simple feed- forward, i.e., a look-up table of orbit corrector settings as a function of insertion device gaps, will be implemented during these first insertion device tests.

The beam dump procedure needs to be extended, taking into account the insertion devices. At the SLS, we have two modes of beam dump, i.e., the normal dump and the emergency dump. In the former, the insertion device gaps are opened before beam dump while the beam is dumped immediately in the latter. These two modes will be also implemented here. Afterwards, the stored beam is fully under control, and finally, we will provide first photon beams.

The nominal current beam is not essential during phase 6. Therefore, if vacuum conditioning is not sufficient at the end of phase 5 and the beam lifetime is too short, we can proceed to phase 6 with a lower current beam.

Phase 7 - Finalization

In the last phase, the goal is to make the machine ready for the photon beamline commissioning. We will extend the feedforward table to include photon BPMs and storage ring linear coupling. If the multi-bunch feedback was not essential in phase 5, it will be studied at this stage. The commissioning of the beam size monitor will be continued. In as far as time permits, the previous commissioning steps will be refined. Further refinements will follow during the beamline commissioning.

Remarks

The vacuum scouring requires an integrated beam current of 100 A-hours and should ideally be finished after three months, i.e., at the end of dedicated accelerator commissioning. Phase 1 for the injector and the transfer line may take 2 weeks or so (excluding linac commissioning). Therefore, we have approximately two and half months left. This imposes a condition that the average beam current should be about 55 mA or higher. This condition seems achievable but indicates that the activities to increase the beam current are priority. Therefore, we have to follow completely the above commission steps towards achieving the first photon beam.

The commissioning will be interrupted with important radiation measurements, and the machine at the end of commissioning has to meet the radiation safety regulations. For instance, the beam lifetime should be sufficiently long to limit radiation levels. Our target is an operation condition similar to the SLS, where the beam lifetime is typically more than 8 hours.

References

- [1.01] L. Farvacque et al., A low emittance lattice for the ESRF, IPAC Shanghai, China, 2013.
- [1.02] P. Raimondi, priv. comm., 2020.
- [1.03] J. Bengtsson & A. Streun, Robust design strategy for SLS 2.0, SLS2-BJ84-001-2, 2017.
- [1.04] M. Böge et al., Correction of imperfection in the SLS storage ring, PAC Vancouver, Canada, 2009.
- [1.05] M. Aiba, Non-linear optics correction, SLS2-AM81-005-1, 2020.
- [1.06] J. Kallestrup and M. Aiba, Emittance exchange in electron booster synchrotron by coupling resonance crossing, Phys. Rev. Accel. and Beams 23, 020701, 2020.
- [1.07] D. Shuman et al., Stray field reduction of ALS eddy current septum magnets, PAC Knoxville, USA, 2005.
- [1.08] M. Aiba and A. Streun, SLS 2.0 injection and injection straight layout, SLS2-AM81-003-4, 2021.
- [1.09] M. Böge et al., SLS vertical emittance tuning, IPAC San Sebastián, Spain, 2011.
- [1.10] A. Streun, SLS 2.0 Booster-to-Ring Transfer Line, SLS2-SA81-008-5, 15.3.2021.
- [1.11] M. Aiba & A. Streun, "Heilige Liste" SLS 2.0, SLS2-SA81-005-25,17.3.2021.
- [1.12] SLS magnet type data, http://ados.web.psi.ch/slsdesc/optic/typeData.dat.txt
- [1.13] M. Aiba, Beam commissioning Plans and supporting simulations, SLS2-AM81-006 (2020) (under preparation).
- [1.14] M. Böge, Orbit and optics corrections, Presentation Machine Advisory Committee (2020), https://indico.psi.ch/event/9056/contributions/25244/attachments/17092/25073/MAC2020_michael.pdf